Actinyl Chemistry at the Centre for Radiochemistry Research

I. May,[*] R. Copping,[*] S.M. Cornet,[*] M.P. Redmond,[*] C.A. Sharrad,[*] C.E. Talbot-Eeckelears,[*] C.J. Jones,[†] M.J. Sarsfield[†] and R.J. Taylor [†]

[*]Centre for Radiochemistry Research, School of Chemistry, University of Manchester, Oxford Road, Manchester, M13 9PL.
[†]Nexia Solutions, Sellafield, Seascale, Cumbria, CA20 1PG, UK

THE ACTINYL CATIONS

The linear dioxo actinyl cations, $\{AnO_2\}^{x+}$ (x = 1 or 2), dominate the +V and +VI solution chemistry of the mid actinide elements (U, Np, Pu and Am). Usually, between 4-6 additional ligands coordinate in the equatorial plane yielding bipyramidal geometry. An increased understanding of actinyl chemistry will underpin a range of nuclear applications, from novel fuel processing technologies through to environmental waste remediation. Of particular relevance are $\{UO_2\}^{2+}$ and $\{NpO_2\}^{+}$, the dominant chemical forms of U and Np respectively, and $\{PuO_2\}^{+}$, which is thought to have environmental significance.

By far the most commonly studied actinyl cation is $\{UO_2\}^{2+}$, primarily due to its chemical stability and the comparatively low radiological hazard associated with uranium chemical research. Recent highlights include the incorporation of this moiety into liquid crystals,[1] the preparation of uranyl selenate nanotubules[2] and structural evidence for cation-cation interaction.[3] Although prone to disproportionation, there are still ongoing investigations into $\{UO_2\}^{+}$ chemistry, including the structural characterisation of $[UO_2(OPPh_3)_4](OTf)$.[4] Finally, bis-imido analogues of the uranyl(VI) cation, $\{U(NR)_2\}^{2+}$, have recently been synthesised and used to probe the role of the 5f and 5d U orbitals in bonding.[5]

The higher specific activity of the transuranium elements restricts experimental chemistry to specialist facilities. While there have been quite a few neptunyl (V and VI) structural studies the first structural characterisation of $\{PuO_2\}^{2+}$,[6] and indeed $\{PuO_2\}^{+}$,[7] complexes have only just been reported. This lack of basic knowledge is also reflected in solution chemistry, with a recent report on $\{PuO_2\}^{2+}$ hydrolysis providing valuable thermodynamic data.[8] Perhaps the most interesting recent development in neptunyl chemistry has been the synthesis of $\{NpO_2\}^{+}$ (and indeed $\{UO_2\}^{2+}$) peroxide nanoclusters from alkaline peroxide solution.[9] Finally, while there is no spectroscopic or structural evidence for $\{PaO_2\}^{+}$ a recent EXAFS study points to the existence of a Pa(V) single oxo species, $\{PaO\}^{3+}$.[10]

ACTINYL CHEMISTRY AT THE CENTRE FOR RADIOCHEMISTRY RESEARCH

At the Centre for Radiochemistry we have investigated several actinyl systems. Recent highlights include the use of spectroscopic techniques to prove that the pertechnetate anion, $[TcO_4]^{-}$, can coordinate directly to the uranyl(VI) cation[11] and that bioreduction of $\{UO_2\}^{2+}$ to U(IV) can occur via a $\{UO_2\}^{+}$ intermediate.[12] Tri-lacunary heteropolyoxometalate ligands have been shown to be very good complexants for the uranyl cation and we have used comparatively straightforward synthetic strategies to take this chemistry forward to neptunyl(V).[13] Very recently we have made significant advances in this area of research, yielding further structural

and spectroscopic characterisation of $\{NpO_2\}^+$ complexes with different tri-lacunary ligands (see, for example, Fig. 1) and extending our investigations to $\{NpO_2\}^{2+}$ and $\{PuO_2\}^{2+}$. Both the charge on the actinyl cation (*e.g.* $\{NpO_2\}^+$ *vs* $\{NpO_2\}^{2+}$) and the type of polyoxometalate anion (*e.g.* A-type *vs* B-type) can lead to different structural types of complex being isolated.

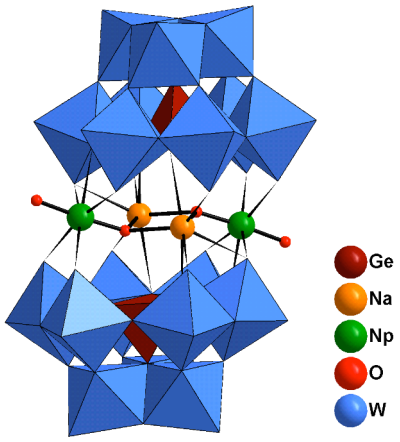

Fig. 1 Polyhedra representation of $[Na_2(Np^VO_2)_2(GeW_9O_{34})_2]^{16-}$

Focusing again on uranyl chemistry, non-aqueous systems have been investigated where the ligands have been chosen with the aim of perturbing the actinyl bond. As an example of this chemistry bidentate (NCN) benzaminato ligands, $[PhC(NSiMe_3)_2]^-$, can be used to complex to $\{UO_2\}^{2+}$ and significantly distort (bending and stretching) the uranyl cation. Using this ligand system the uranyl oxygen can be activated to behave as a Lewis base, yielding the $B(C_6F_6)_3$ adduct, $[UO_2B(C_6F_5)_3\{(SiMe_3N)CPh(NSiMe_3)\}_2]$.[14] We have recently taken this chemistry transuranic, showing that $R_3P{=}NH$ ligands will displace $R_3P{=}O$ ligands coordinated to $\{UO_2\}^{2+}$ and $\{NpO_2\}^{2+}$.[15]

Our current research goal is to further develop transuranic actinyl research. This will be undertaken experimentally in collaboration with Nexia Solutions at Sellafield and EU ACTINET partner laboratories; particularly ROBL-ESRF, Grenoble and CEA Atalante at Marcoule. A collaborative computation programme is currently being undertaken by Kaltsoyannis and co-workers at University College London.

1 T. Cardinaels, J. Ramaekers, D. Guillon, B. Donnio and K. Binnemans, J. Amer. Chem. Soc. **127**, 17602 (2005).
2 S.V. Krivovichev, V. Kahlenberg, I.G. Tananaev, R. Kaindl, E. Mersdorf and B.F. Myasoedov, J. Amer. Chem. Soc. **127**, 1072 (2005).
3 T.A. Sullens, R.A. Jensen, T.Y. Shvareva and T.E. Albrecht-Schmitt, J. Amer. Chem. Soc. **126**, 2676 (2004).
4 J-C. Berthet, M. Nierlich and M. Ephritikhine, Angew. Chem. Int. Ed., **42**, 1952 (2003).
5 T.W. Hayton, J.M. Boncella, B.L. Scott, P.D. Palmer, E.R. Batista and P.J. Hay, Science, **310**, 1941 (2005).
6 W. Runde, A.C. Bean, T.E. Albrecht-schmitt and B.L. Scott, Chem. Commun. 478 (2003).
7 A.A. Bessonov, M.S. Grigoriev, I.A. Charushnikova and N.N. Krot in *Recent Advances in Actinide Science*, edited by R. Alvares, N.D. Bryan and I. May [Royal Society of Chemistry, in press].
8 S.D. Reilly and M.P. Neu, Inorg. Chem., advanced article (2006).
9 P.C. Burns, K-A. Kubatko, G. Sigmon, B.J. Fryer, J.E. Gagnon, M.R. Antonio and L. Soderholm, Angew. Chem. Int. Ed. **44**, 2135 (2005).
10 C. Le Naour, D. Trubert, M.V. Di Giandomenico, C. Fillaux, C. Den Auwer, Ph. Moisy and C. Hennig, Inorg. Chem. **44**, 9542 (2005).
11 A.D. Sutton, G.H. John, M.J. Sarsfield, J.C. Renshaw, I. May, L.R. Martin, A.J. Selvage, D. Collison and M. Helliwell, Inorg. Chem. **43**, 5480 (2004).
12 J.C. Renshaw, L.J.C. Butchins, F.R. Livens, I. May, J.M. Charnock and J.R. Lloyd, Environ. Sci. Technol. 39, 5657 (2005)
13 A.J. Gaunt, I. May, M. Helliwell and S. Richardson, J. Amer. Chem. Soc. **124**, 13350 (2002).
14 M.J. Sarsfield and M. Helliwell, J. Amer. Chem. Soc., **126**, 1036 (2004).
15 M.J. Sarsfield, I. May, S.M. Cornet and M. Helliwell, Inorg. Chem. 44, 7310 (2005).

Thermodynamic Features of Lanthanide and Actinide Solvent Extraction Reactions

K. L. Nash

Chemistry Department, Washington State University, PO Box 644630, Pullman, WA 99164-4630 (e mail, knash@wsu.edu)

The transuranium actinides were unknown on earth until the late 1930s - early 1940s. From that time through the 1950s and into the 1960s, these elements were discovered as byproducts of the irradiation of uranium (and subsequently of transuranic element targets) with subatomic particles. Separations chemistry (precipitation/co-precipitation, ion exchange, and solvent extraction) was central to the discovery of the individual actinides, to the isolation and purification of target nuclides and to the preparation of samples of sufficient purity to allow elucidation of their chemical/physical properties. Further, solvent extraction, in the form of the PUREX process, has become the single most important separations process in actinide technology.

As we move into the 21st Century, a reinvigoration of actinide separation process chemistry is in evidence. A more wide spread adoption of a closed nuclear fuel cycle approach to radioactive materials management seems inevitable. In fact, a considerable amount of research has been done around the world to develop more efficient separations methods during the last decade. In the future pyrometallurgical/electrometallurgical separations and perhaps more advanced techniques based on volatility or new materials like supercritical fluids or Room Temperature Ionic Liquids may become more important. For the present and the near future, development of new methods continues to rely on the proven techniques of solvent extraction and related methods. This emphasis arises to a significant degree from the considerable amount of insight we have gained into the chemical processes that control solvent extraction processes. The flexibility available in solvent extraction that allows ready adjustment of operational parameters and the inherent adaptability of solvent extraction to continuous operations (and thus high throughput) also favor (and justify) continuation of this dominance.

While both favorable thermodynamics and kinetics are needed for the development of a useful separation technique, the greatest insight into process and new reagent design has been gained from correlations of thermodynamic data describing liquid-liquid phase transfer reactions. Solvent extraction reactions of f elements range widely from enthalpy- to entropy stabilized. Enthalpy-entropy compensation effects and solvation energy differences also figure prominently in this chemistry. It is important to note as well that minor differences in the energetics of chemical reactions in solvent extraction can have a major impact on separation efficiency. In this presentation, the basic thermodynamics of solvent extraction reactions of actinide and lanthanide metal ions will be discussed.

Synthesis of new mixed actinides oxalates as precursors of actinides oxide solid solutions

B. Arab-Chapelet[*], S. Grandjean[*] G. Nowogrocki[†] and F. Abraham[†]

[*]Commissariat à l'Energie Atomique, Nuclear Energy Direction, Radiochemistry and Process Division, Valrhô Research Center, BP 17171, 30207 Bagnols sur Ceze, France
[†]Laboratoire de Cristallochimie et Physico-Chimie du Solide, UMR CNRS 8012, ENSCL-USTL, BP 108, 59652 Villeneuve d'Ascq, France

INTRODUCTION

The main objectives of the development of innovative fuel cycles such as those conceived in the Generation IV forum, are an efficient use of energetic resources by recycling together the major and valuable actinides such as uranium and plutonium, and a drastic decrease of the radiotoxicity of the ultimate wastes by partitioning and transmutating the minor ones such as americium, curium or neptunium. Whatever the choice of management in the present or future, innovative synthesis methods are studied to elaborate new mixed actinides based materials. For their synthesis, wet methods fulfill very useful requirements such as flexibility, compatibility with a hydrometallurgical fuel processing, less dissemination of highly radioactive dusts during processing, and above all a better accessibility to very homogeneous polymetallic compounds and interesting nanostructures[1]. Moreover these homogeneous solids improve the proliferation resistance by diluting plutonium with other actinides.

The oxalic precipitation of plutonium(IV) or plutonium(III) is used at an industrial scale during the reprocessing of the nuclear fuel, e.g. by the PUREX process[2], in order to convert into oxide this energetically valuable actinide. Oxalic acid is also a very common reagent to recover actinides from liquid waste using precipitation methods because of the very low solubility of An(IV) or An(III) oxalate compounds in acidic solutions[3,4]. The flexibility of the oxalate ligand leads to actinides-based solid compounds which are particularly suitable precursors of actinides oxide solid solutions.

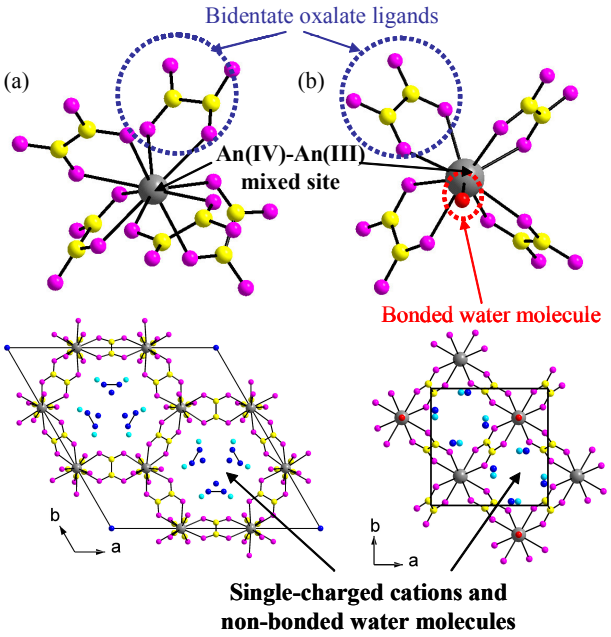

Fig 1: Environment of An(IV) – An(III) crystallographic mixed site and structural arrangement in : the hexagonal mixed oxalate (a) and in the tetragonal one (b).

AN(IV)-AN(III) OXALIC COCONVERSION

Reaction of a solution containing a tetravalent actinide An(IV) and a trivalent actinide An(III) in presence of oxalic acid in acidic media under controlled conditions, leads

to the precipitation of mixed An(IV)-An(III) oxalate compounds, with An(IV)=Th, Np, U or Pu and An(III)=Pu or Am, never described before. New mixed An(IV)-An(III) single–phase co-precipitates were obtained and characterized from powder diffraction patterns by analogy to uranium (IV)-lanthanide (III) oxalates whose structures were solved recently from single-crystal X-ray diffraction data[5,6,7]. By varying the (An^{IV},An^{III}) pair and depending on the An^{IV}/An^{III} ratio, two original series were identified, $M_{2+x}An^{IV}_{2-x}An^{III}_{x}(C_2O_4)_5 \cdot 4H_2O$ (**1**) and $M_{1-x}[An^{III}_{1-x}An^{IV}_{x}(C_2O_4)_2.H_2O] \cdot 4H_2O$ (**2**) (M = single charged cation), with hexagonal or tetragonal symmetry, respectively. The originality of both structures is based on a mixed crystallographic site which can accept either a tetravalent actinide or a trivalent one, the charge balance being ensured by the adjustment of the single-charged ions within the structure. The main difference is that actinides are ten-coordinated in (1) and nine-coordinated in (2) (Fig 1). The honeycomb-like structure of the hexagonal compound is based on a three dimensional network of metallic and oxalate ions creating parallel tunnels. For the tetragonal series, the metallic ions are linked through oxalates ions to build a bidimensional arrangement of squared cycles.

Complementary investigations by UV-visible and Infrared spectroscopies and thermogravimetric analysis were led (Fig 2). They confirm the simultaneous co-precipitation of An(III) and An(IV) without modification neither of the ratio between A(IV) and An(III) nor of the oxidation state and highlight the role of single-charged cation and water molecules.

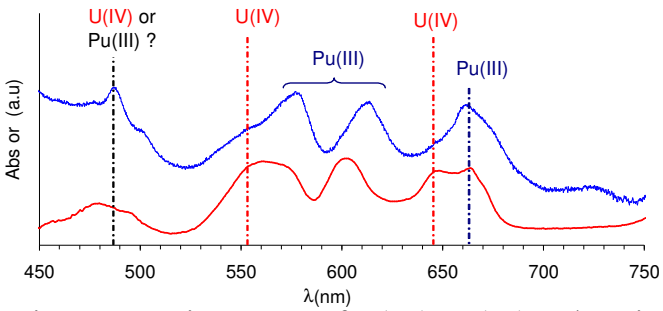

Fig 2 : UV-Vis Spectra of U(IV)-Pu(III) 50/50 nitric solution (red line) and U(IV)-Pu(III) solid co-precipitate showing the invariability of oxidation state during experiment.

CONCLUSION

In these experiments dedicated to actinides co-management using oxalic co-conversion, the simultaneous co-precipitation of the involved actinides is an important first achievement considering the specific properties of each actinide, properties which moreover differ according to various possible oxidation states.

---

[1] S. Pillon, J. Somers, S. Grandjean, J. Lacquement, J.of Nucl. Mater., **320**, 36-43, (2003).
[2] F. Drain, B. Gillet, G. Bertolotti, «Oxalate process: the unique way for plutonium conversion», GLOBAL 1999 International Conference.
[3] R.D. Bhanushali, *et al.,* J. Radioanal. Nucl. Chem.**, 240**, N°2, 631-635, (1999).
[4] P.P Mapara, *et al*., *J.* Radioanal. Nucl. Chem.**, 240**, N°3, 977-979, (1999).
[5] B. Chapelet-Arab, S. Grandjean, G. Nowogrocki et F. Abraham., J. Solid State Chem., **178**, 3046-3054, (2005).
[6] B. Chapelet-Arab, S. Grandjean, G. Nowogrocki et F. Abraham, J. Solid State Chem., **178**, 3055-3065,(2005).
[7] B. Chapelet-Arab, L. Duvieubourg, F. Abraham, G. Nowogrocki et S. Grandjean, submitted to: J. Solid State Chem.,, (2006).

Methods of Separations of Transuranium Elements Based on the Complex – Formation Ligands: Extraction and Sorption

B.F. Myasoedov[†], Yu.M. Kulyako[†], I.G. Tananaev[†], V.V. Yakshin[*], A.Yu. Tsivadze[*]

[†] Vernadsky Institute of Geochemistry and Analytical Chemistry Russian Academy of Science, Moscow 199991 Russia

[*] Frumkin Institute of Physical Chemistry and Electrochemistry Russian Academy of Science, Moscow 199991 Russia

INTRODUCTION

The problem of high radioactive waste (HLW) treatment and storage is at present one of the most important ecological problems in Russia and in the U.S. Solution to this problem have two general aspects: (1) development of effective methods of HLW partitioning and disposal; and (2) determination, recognition, and isolation of hazardous radionuclides in the Environment. To satisfy both of these demands the main question is choice of highly accurate methods of radionuclide recognition, separation, and recovery of long-live isotopes from complex media. In practice for these purposes an extraction and sorption methods are used. In our opinion the following directions in the frame of development of fundamental knowledge of the processes of separation in nuclear technology will predominate in 21-st century: (1) The directed design and study of selective macro cyclic ionophores and another ligands with high chemical and radiolytic stability for isolation of a long-live radionuclides by means of a Liquid-Liquid, and Countercurrent Chromatography (CCC) from different media; (2) Practical realization of Supercritical Fluid Extraction (SFE) method based on quantitatively dissolution of UO_2 in some organic reagents, saturated with nitric acid in supercritical CO_2 as a solvent; (3) Development of effective sorption methods of reducing and recovery of Pu and other TRU from different man-caused and nature solutions using a fibrous "filled" sorbents. The results of a systematic study on realization of these three directions are summarized in our presentation.

EXPERIMENTAL

Extraction of U, and TRU by (4,4'(5')) bis(dialkylphosphoryl)-, bis(diphenylphosphoryl)-, bis(O-alkyl)phosphoryl)-benzo-n-crown-m ethers (n = 18 and m = 6; n = 21 and m = 7; n = 24 and m = 8, respectively) solutions in 1,2-dichloroethane and chloroform has been studied from nitric acidic media. It has been demonstrated that, during extraction, distribution coefficients (D_M) of U(VI), Pu(IV), Am(III), Eu(III) depend upon experimental conditions as well as upon structural features of the molecular complexes used. It is important that, within the range of $[HNO_3]$ = 0,02 – 1,0 mol/l, the D_M values for metals depend on stereochemical orientation of phosphoryl- groups. It was found out that the extraction ability of cis(4,4'-) isomers is higher than for trans(4,5'-) isomers and for their mixtures. Using compound that has cis-oriented $(nBuO)_2P(O)$-groups as an example, it was observed that the highest D_U = 0,98 in 3 mol/l HNO_3; D_{Pu} = 5,1 in 0,5 mol/l HNO_3 and D_{Am} = 0,007 at pH = 2. For trans-conformer under the same conditions D_M for U(VI), Pu(IV), and Am(III) are 0.091, 1.8; 0.003, respectively. It has been shown by using the BIO+(CHARMM) and MNDO computer methods, that the complexes of elements with trans-positions of the $(nBuO)_2P(O)$- groups have larger volume, their energy

of formation is higher, and stability of the „host-guest“ complexes is lower All this leads to the decrease of the D_M value during extraction. Under the same other conditions, the influence of the dimensions of the macrocycle (C_n) upon extraction is essential. Using extraction of Am(III) from 0.01–3MHNO_3 as an example, it has been demonstrated that for all molecules investigated, the most effective extragents are crown-ethers with n = 21. The shift of the D_{Am}^{max} to the higher [HNO_3] was observed with the increase of n. The sequence of the coordination properties of phosphoryl-containing ligands based upon functionalized benzo-21-crown-7 under extraction of Am(III) from 0.01–3M HNO_3 is as follows: (nBuO)(OH)P(O)- >> $(nBuO)_2P(O)$- > $Ph_2P(O)$-. Extraction properties of di(nBuO)(OH)P(O)-dibenzo-21-crown-7 (D_{Am} = 814 in 0,1M HNO_3) are $>10^2$ higher for all compounds studied. The conditions of selective separation of Am(III)/Eu(III) by means of bis(O-alkyl)(OH)phosphoryl)-dibenzo-21-crown-7 have been determined with separation factor of >90 at [HNO_3] = 0.01 mol/l.

Application of SFE technique was recently shown to be very promising for oxide nuclear fuel reprocessing thanks to using supercritical CO_2. The main aim of realization of this process is to find and study the necessary organic ligands suitable for direct dissolution of TRU oxides for their separation. For experiments the adducts TBP-HNO_3 (**1**), methylisobutylketone - HNO_3 (**2**) and dimethyl-N,N’-dioctyl-hexylethoximalon- amide - HNO_3 (**3**) are prepared by mixing of equal volumes of the ligands with 8M HNO_3 during 15 min. The known volume of adducts used were introduced into a centrifuged test-tubes with the MOX samples (90-95% $^{233+238}UO_2$, and 10-5% $^{239}PuO_2$) at 60^0C for ~3 h for dissolution. It was shown that MOX completely dissolved only in the (**1**) and (**3**) (>99% of U, and Pu in the solution). When dissolving the MOX sample in the (**2**), extraction of U only occurs (>99%), resulting in separation of U(VI) from Pu(IV), which remains (>99%) in the solid phase probably as PuO_2. Hence, the system (**2**) one can find application in the future technology of oxide nuclear fuel reprocessing under SFE.

Direct dissolution of solid solution of 4.6% of PuO_2 and 95.5% of UO_2 in TBP-HNO_3 complex, conducted by us previously, requires the subsequent separation of U and Pu. Such separation may be performed by the method of CCC with the use of two-phase liquid system of TBP-HNO_3. Influence of compositions of mobile and immobile phases on efficiency of separation of the elements was studied, and it was shown that CCC permits to separate U and Pu rather effectively under the conditions of concentration gradients both of TBP in immobile phase and of HNO_3 in mobile phase. At first, under optimal separation conditions, the fraction containing 99.7% of Pu and 0.3% of U goes out, and then uranium fraction is eluted.

At detection of TRU in natural and technological waters it is required their pre-concentration and separation from other elements. For this purpose it is most perspective sorption separation of TRU with use of the fibrous "filled" sorbents. These materials represent thin porous fibers inside which it is kept fines grain “filler” – complex forming or ion exchanger sorbent. We investigated the properties of the fibrous "filled" sorbents type POLYORGS 33-n, 34-n, and 35-n (complexing sorbents with amidoxime and hydrazidine groups) for pre-concentration of Pu(IV), U(VI), Np(V), Am(III) (~10 ppm) from solutions: **I**- 0.5M NaCl, pH=6; **II**- Ca-0.043; Mg-0.08; Na-0.045; Cl- 0.2 mg/l; pH=6.5; **III**– Ca- 42; Mg-10; Na-54; K-39; Cl-4.6; SO_4-29; HCO_3^- - 159 mg/l. It was found that the sorption degree of the TRU used during extraction from all the model solutions by POLIORGS at ratio V : M = 100 ml/g and time contact ~2 h are exceeded 96 – 99%.

The work was supported by the U.S.DOE-OBES, Project RUC2-20010-MO-04, RFBR grant 05-03-32908, 33094; and President RF grant 1693.2003.3.

Plutonium and Other Actinides Behaviour in NEXT Process

S. Miura, M. Nakahara, Y. Sano, M. Kamiya, K. Nomura, J. Komaki

Japan Atomic Energy Agency, Tokai, Ibaraki, 319-1195, JAPAN

INTRODUCTION

In the feasibility study on the commercialized fast reactor cycle systems, which aims for ensuring safety, economical competitiveness, efficient utilization of resources, proliferation resistance, and decreasing environmental burden, Japan Atomic Energy Agency (JAEA) has been developing the advanced aqueous reprocessing system named "New EXtraction system for TRU recovery (NEXT) process" for the spent fast reactor fuel reprocessing. The NEXT process basically consists of 3 characteristic processes; the crystallization process for recovering a part of U from dissolver solution, the U-Pu-Np co-recovery process with single cycle flowsheet using TBP as an extractant and the Am-Cm recovery process with extraction chromatography[1]. In this study, we will discuss the behaviour of Pu and other actinides in the crystallization process and the U-Pu-Np co-recovery process with referring to the experimental results obtained in our experimental facility, Chemical Processing Facility (CPF).

CRYSTALLIZATION PROCESS

As we reported in the previous work[2], Pu shows the different behaviour in the crystallization process according to its valence in the dissolver solution. If Pu(VI) exists in the dissolver solution, Pu is co-crystallized with U, which brings low decontamination factor (DF) of Pu to U (DF_{Pu}) and makes it difficult to improve DF_{Pu} by washing the crystal. On the other hand, under the condition that Pu is adjusted to Pu(IV) in the dissolver solution, Pu is not crystallized and only U crystal is obtained. Although the surface of the U crystal is contaminated with mother solution containing Pu, comparatively high DF_{Pu} can be achieved easily by washing the crystal surface with nitric acid solution. It is, therefore, important for preventing Pu co-crystallization and keeping high DF_{Pu} to adjust the Pu valence to Pu(IV) in the dissolver solution.

Photo 1: U crystal obtained in the crystallization tests with U-Pu-Cs solution (U: 409g/l, Pu(IV): 41.8g/l, Cs: 4.6g/l) (after washing). A small amount of whitish green crystals are observed in the yellow U crystal.

Under some crystallization condition, we have found that Cs contained in the dissolver solution as FP can be hardly separated from the U crystal, i.e. DF_{Cs} shows very low values[3]. In our recent research, it is suggested that such behaviour of Cs will be related with the formation of some kinds of Cs compounds with Pu

in the dissolver solution. It is known that whitish green crystal of $Cs_2Pu(NO_3)_6$ is composed by mixing $CsNO_3$ and $Pu(NO_3)_4$ in high nitric acid solution under low temperature condition. We have also obtained a small amount of similar crystals in the U crystal after some crystallization tests in which the concentration of Cs is comparatively high (Photo 1).

The analysis of these crystals is now in progress, and it will be further required for high DF_{Cs} to clarify the process condition without the formation of such Cs-Pu compounds, and/or to develop some purification methods for the U crystal contaminated with these compounds.

U-Pu-Np CO-RECOVERY PROCESS

In the U-Pu-Np co-recovery process with single cycle flowsheet, Pu partitioning section is eliminated from the conventional PUREX process, i.e. no Pu reduction to Pu(III) occurs in the process. In this process, Pu is stripped with U just by diluted nitric acid solution. The stripping reactions of Pu (Pu(IV)) and U (U(VI)) are exothermic and endothermic respectively. Therefore, it is important for the effective co-stripping of these elements to control the temperature carefully in the striping section (Fig. 1). It is also required for preventing the generation of Pu polymer under the low acidity to adjust the nitric acid concentration to be a suitable value in the stripping section.

Among the actinide elements, Np shows the complex behaviour in the extraction section because of its variable valences in the nitric acid solution; extractable Np(IV) and Np(VI), and inextractable Np(V). These Np valences are affected by the concentration of nitric acid and nitrous acid in the process, and it is desirable for the effective Np extraction, i.e. the effective oxidation of Np to extractable Np(VI) in the extraction section, to increase the nitric acid concentration, and to control and optimize the nitrous acid concentration in this section.

Although there are some considerable points on developing and improving the flowsheet for the U-Pu-Np co-recovery process as mentioned above, we have confirmed that over 99.9% of U and Pu, and 99% of Np can be co-recovered with sufficient DF of total γ (~10^4) under the appropriate condition[4,5]. For optimizing the flowsheet, further investigation will be carried out.

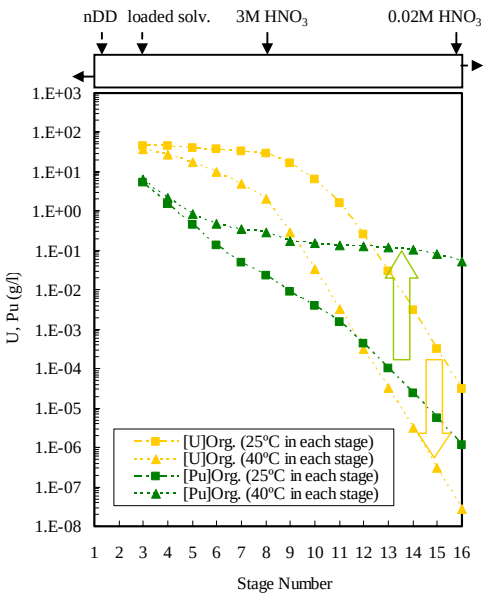

Fig. 1: Temperature dependence of U and Pu profiles in the stripping section, which was calculated with the simulation code "MIXSET-X".

1 Y. Takata, *et al.*, J. Nucl. Sci. Technol., 41(3), **307** (2004).
2 K. Yano, *et al.*, *Proc. of Actinides2005*, **5P47** (2005).
3 K. Yano, *et al.*, *Proc. of Global2005*, **118** (2005).
4 Y. Sano, *et al.*, *Proc. of ISEC2005*, **B206** (2005).
5 M. Nakahara, *et al.*, *Proc. of Global2005*, **262** (2005).

Electrochemical studies on Plutonium in molten salts

G. Bourgès[*], S. Rochefort[*], D. Lambertin[*], H. Chollet[*], S. Delpech[†], G. Picard[†]
[*] CEA – Centre d'études de Valduc – 21 120 Is sur Tille – France,
[†] Laboratoire d'Electrochimie et de Chimie Analytique - ENSCP, 11 rue Pierre et Marie Curie - 75231 Paris - France

INTRODUCTION

Pyrochemical separations, involving salt and metal molten media, by liquid/liquid extraction or electrorefining are studied for nuclear defence and civil applications. Both are concerned by actinides separations. Lanthanides, such as cerium, are often used as surrogates.

Early steps of such pyrochemical processes development consist of studying of the molten salt chemistry of the elements to be separated. Activity coefficients of the solute in liquid metal and salt phases are important thermochemical parameters for predicting separation efficiency and to assess the solvents influence.

CEA has been operating such processes in chloride media for more than 40 years for both plutonium metal preparation and residues recovery. In the 70's, the earlier studies concerned plutonium in NaCl/KCl/$BaCl_2$ mixture. More recently, Pu(III) has been investigated in NaCl/KCl eutectic mixture and in pure $CaCl_2$ .As solvent metal such as gallium could have potentialities for the recovery of plutonium from metal scraps, the thermochemical properties of plutonium dissolved in gallium were then studied.

EXPERIMENTAL

Electrochemical investigations using cyclic voltammetry, potentiometry and chronoamperometry have been carried out to study the properties of plutonium (III) in various molten chlorides and of Pu metal in gallium metal.

The feed chlorides were previously dried. Pure commercial gallium and plutonium metal pieces prepared at CEA/Valduc were used as metal feed. The chloride salt and the metal were melted in a magnesia crucible placed under dry argon. The reference electrode was a silver wire dipped into a porous alumina tube containing a solution of silver chloride in the corresponding chloride. Tungsten wires were used as working and counter electrodes.

ELECTROCHEMICAL PROPERTIES OF PLUTONIUM IN MOLTEN CHLORIDES

The standard potential of Pu(III)/Pu redox couple in eutectic mixture of NaCl/KCl/$BaCl_2$ at 1073 K deduced from early studies by potentiometry is equal to -2.56 V[1](see fig.1). In NaCl/KCl eutectic mixture and in pure $CaCl_2$ (see fig.2), the standard potential deduced from cyclic voltammetry are respectively -2.54 V and -2.51 V, and led to the activity coefficients of Pu(III) in the molten salt[2]. In NaCl/KCl media, the presence of plutonium seems to involve a decrease of the solvent limit (sodium reduction) so that the gap between Pu^{3+}/Pu and Na^{+}/Na couples is small. In more acidic melt, like $CaCl_2$, the standard potential is close to the reference related to pure compounds.

As oxides ions concentration in molten salts may be important for separation processes, the potential – p(O^{2-}) diagrams were built from these results and literature data in order to define the stability domains of the plutonium – oxygen - chlorine compounds[2,3].

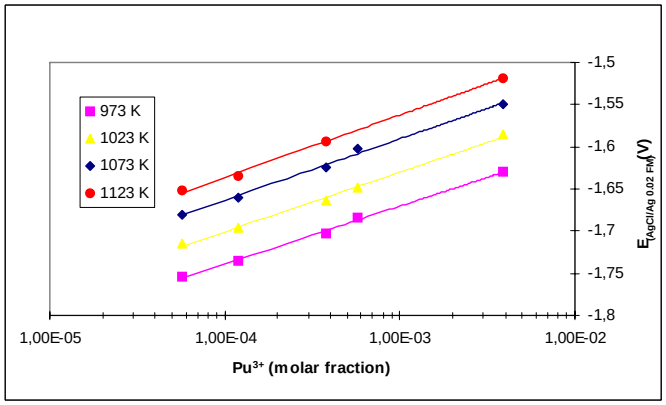

Fig. 1: Potentiometry of Pu(III)/Pu couple in NaCl/KCl/$BaCl_2$ (from[1]).

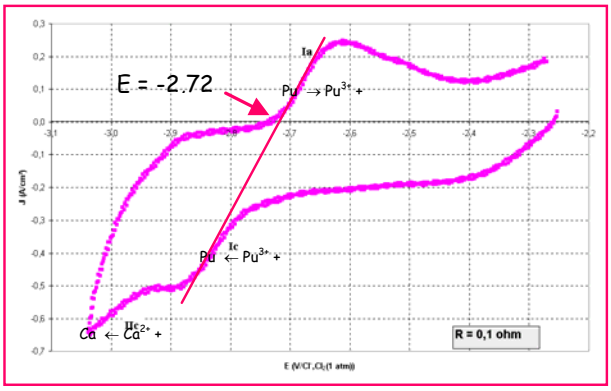

Fig. 2: Cyclic voltammetry obtained on a tungsten working electrode in $CaCl_2$ containing Pu(III) ions ($X_{Pu(III)}$ = 1.1x 10^{-3})

THERMOCHEMICAL PROPERTIES OF PLUTONIUM IN LIQUID GALLIUM

Chronoamperometry on plutonium in liquid gallium in chlorides – $CaCl_2$ (see fig. 3) and equimolar NaCl/KCl - led to the determination of the activity coefficient of Pu in liquid Ga, log γ = - 7,2[4].

This new data is key parameter to assess the scientific feasibility of an original process for plutonium recovery from metallic scraps after dissolution in liquid gallium by selective extraction.

As activity coefficient of cerium in gallium was previously determined[4], it is possible to compare gallium with other solvent liquid metals such as Cd, Bi, Al for plutonium - cerium separation.

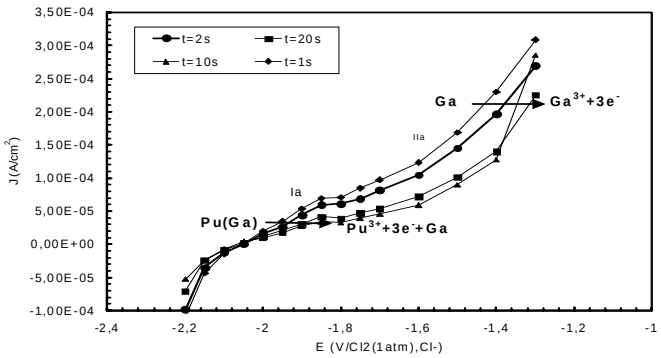

Fig. 3: Intensity-potential curve in $CaCl_2$ at 1073K obtained from chronoamperograms, XPu(Ga)=0.0129 ,$XPuCl_3$=0.0011

The authors would like to thank J. Lannaud for his "pioneer" studies, and staff of Valduc 118 facility for their technical support.

1 J. Lannaud, CEA-DAM internal report (1973).
2 D. Lambertin, S. Ched'Homme, G. Bourgès, S. Sanchez, G. Picard, J. of Nuclear Materials, 341, (2005), 124-130
3 S. Sanchez, G. Picard, D. Lambertin, J. Lacquement, Proceedings "OCDE/NEA workshop on pyrochemical separations", Avignon, (14-16 march 2000), 213-221
4 D. Lambertin, S. Ched'Homme, G. Bourgès, S. Sanchez, G. Picard, J. of Nuclear Materials, 341, (2005), 131-140

Systematics in $PuTGa_5$ Compounds

F. Wastin, E. Colineau, F. Jutier and J. Rebizant

*European Commission, Joint Research Centre, Institute for Transuranium Elements, Postfach 2340, D-76125 Karlsruhe, Germany

The recent discovery of superconductivity[1,2] at a high transition temperature in the plutonium-based compounds $PuCoGa_5$ (T_c = 18.5 K) and $PuRhGa_5$ (T_c = 9 K) has ignited a high interest in these new materials. Prior to this discovery, no Pu-based compound was found to exhibit superconductivity. Moreover, among the known actinide or lanthanide superconductors one rarely finds a material with a T_c over 2 K. From this perspective, Pu(Co or Rh)Ga_5 can be regarded to have an astonishingly high transition temperature and the nature of the superconducting pair formation has been a point of special focus[3,4]. Most recently, experimental studies, employing nuclear magnetic and quadrupolar resonance (NMR, NQR), proved that indeed $PuCoGa_5$ and $PuRhGa_5$ are unconventional, spin-singlet, *d*-wave type superconductors[5,6]. However, the experimental investigations of these Pu-based compounds is complicated by the evolution of their properties as a function of time[1-2,5-7], due to the impact of self-radiation damage, induced by the α-decay of the Pu atoms.

At ITU-Karlsruhe, we have started a systematic investigation of $PuTGa_5$ (T a d transition metal) summarized in the figure 1, but no new superconducting material has been evidenced up to now, and paramagnetic type behaviour is most commonly observed in the series. However some systematics can be drawn out.

3d	**Fe** PP	**Co** 18.6K	**Ni** PP
4d	*Ru*	**Rh** 9K	*Pd*
5d	*Os*	**Ir** PP	*Pt*

Paramagnetic | Superconductor

element in italic: does not form or was not obtained

Fig 1: Behaviour of $PuTGa_5$ compounds.

First, from the chemical point of view, we observe that moving along the 3d series beside the Co and/or going down within the Co-column, the 1:1:5s are more and more difficult to obtain as pure phase and become unstable. Thermodynamic competition with neighbouring phases (e.g. 2:1:8, 4:1:12, …) is more and more 1:1:5 unfavourable. This observation may be related to the 1:1:5 phase stability observed in Ce-compounds (only formed with In) and other 4*f* and 5*f* elements (Th, U, Np) that reveals a marked effect of the *f*-electron count. It is marginal to conclude that the electronic structure may play an important role in the 1:1:5 phase stability and may deserve a thorough theroretical investigation.

Another systematic addresses the interesting variation of the T_c versus *c/a* ratio[8] (Figure 2a). For each family, the differences in T_c from compound to compound (under changes in the doping on the transition metal site) from the group Co, Rh, Ir are found to correlate with the differences in

c/a ratio: the plot of T*c* versus c/a forms a straight line of positive slope. However, recent solid solution studies[9] and high-pressure investigations[10], have shown that this variation could not be assigned to the *c/a* ratio as being the main tuning parameter.

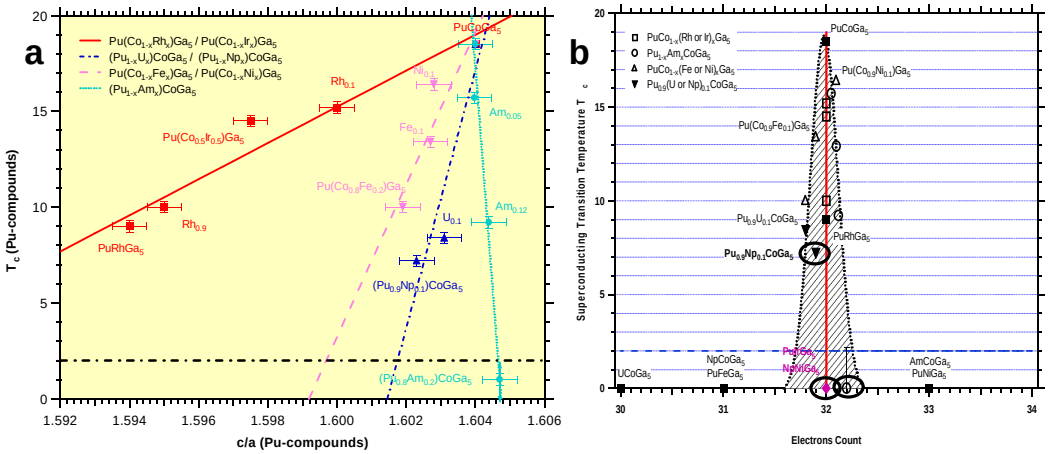

Fig 2: a) Variation of T_c as a function of the c/a ratio and b) Distribution of T_c as a function of the electron counts.

Figure 2b provides a new perspective on the influence of doping the systems investigated with different elements. Plotting the variation of T_c as a function of the electrons count (here only outer-shell electrons are counted), shows a spectacular concentration of all $AnTGa_5$ superconducting compounds in a narrow band at approximately 32±0.2 electrons, whereas all compounds outside of this band (i.e. with different electron count) are not superconducting.

Further systematics, and in particular addressing the magnetic properties, can be drawn and will be addressed in our presentation.

The high purity Pu metals required for the fabrication of the compounds was made available through a loan agreement between Lawrence Livermore National Laboratory and ITU, in the frame of a collaboration involving LLNL, Los Alamos National Laboratory, and the US department of Energy. F. J. acknowledges the European Commission for support in the frame of the Training and Mobility of Researchers" programme.

1 J. L. Sarrao, *et al.*, Nature **420**, (2002).
2 F. Wastin, *et al.*, J. Phys. Condens. Matter **15**, (2003).
3 T. Maehira, *et al.*, Phys. Rev. Lett. **90,** (2003).
4 I. Opahle, P. M. Oppeneer, Phys. Rev. Lett. **90**, (2003).
5 N. J. Curro, *et al.*, Nature **434**, (2005).
6 H. Sakai, *et al.*, J. Phys. Soc. Jpn. **74**, (2005).
7 F. Jutier, , *et al.*, Physica B **359-361**, (2005).
8 E.D. Bauer, *et al.*, Phys. Rev. Lett. **93**, (2004).
9 P.Boulet, *et al.*, Phys. Rev. B **72**, (2005).
10 P. Normile, et al., Phys. Rev. B **72**, (2005).

Probing the Coulomb interaction of the unconventional superconductor $PuCoGa_5$ by phonon spectroscopy

S. Raymond[*], P. Piekarz[†], J.P. Sanchez[*], J. Serrano[‡], M. Krisch[‡], B. Janoušová[◊], J. Rebizant[◊], N. Metoki[ϒ], K. Kaneko[ϒ], P.T. Jochym[†], A.M. Oleś[†,♦] and K. Parlinski[†].

[*]CEA-Grenoble, DRFMC / SPSMS, 38054 Grenoble Cedex, France
[†] Institute of Nuclear Physics, Polish Academy of Sciences, 31342 Krakow, Poland
[‡]European Synchrotron Radiation Facility, 38043 Grenoble Cedex, France
[◊]European Commission, Institute for Transuranium Elements, 76125 Karlsruhe, Germany
[ϒ]Japan Atomic Energy Agency, 319-1195, Tokai, Japan
[♦]Max Planck Institut für Festkörperforschung, 70569 Stuttgart, Germany

Given its characteristic energy scales, the unconventional superconductor $PuCoGa_5$ (T_c =18.5 K) is playing the central role of a missing link between the canonical heavy fermion superconductors and the high-T_c cuprates [1]. The understanding of its physical properties will thus allow progress in the global understanding of unconventional superconductivity. While a magnetic mechanism for the electron pairing is strongly suggested, the study of the phonon spectrum is nonetheless of interest. This is partly due to tremendous recent progresses in band structure calculations that allow to compute accurate phonon spectrum of strongly correlated electron systems [2,3].

We measured the phonon dispersion curves of single crystalline $PuCoGa_5$ samples along the [100], [110] and [001] directions by Inelastic X-ray Scattering (IXS) at room temperature. The IXS data are compared with a density functional theory (DFT) *ab-initio* calculation using the Generalized Gradient Approximation with finite U (GGA+U) method [2]. We concluded that the inclusion of a finite on-site repulsion between f electrons, U, of approximately 3 eV is essential to describe quantitatively the lattice dynamics of $PuCoGa_5$. This conclusion is primarily drawn from the sensitivity of the lowest transverse optic modes to the Coulomb repulsion that undergo up to 30 % change in energy between the calculations with U = 0 and U = 3 eV. The comparison of the experimental data with the *ab-initio* calculation for U = 0 eV and U = 3 eV is

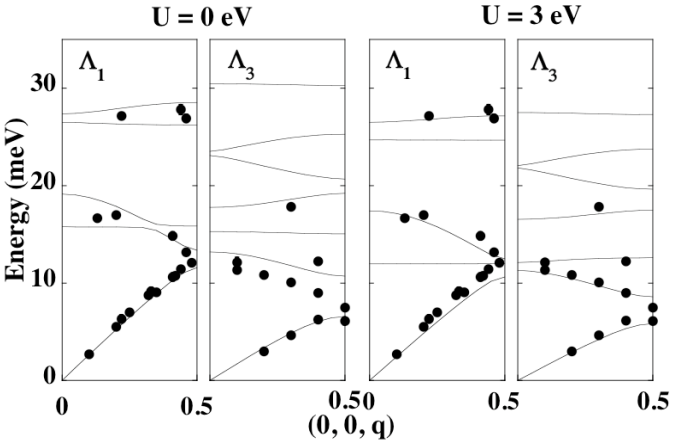

Fig. 1 : Dispersion relation of $PuCoGa_5$ for the [001] direction at 300 K. The experimental data (full circles) are compared with *ab-initio* calculation for U = 0 (left) and 3 eV (right). Branches are classified according to the irreducible representations (Λ_1, Λ_3) along [001].

shown in Fig.1 for the direction [001]. The best agreement with the $U = 3$ eV calculation, that is found for [100], [110] and [001] directions, gives support to the existence of substantial f electrons localization in $PuCoGa_5$ in agreement with photoemission results [4].

In contrast, it was found that the phonon spectrum of the itinerant electron paramagnet $UCoGa_5$ is better described with $U = 0$ eV [5]. This is consistant with the known delocalization of f elec-

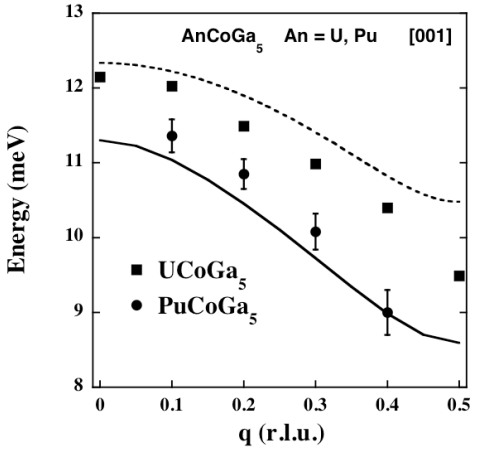

Fig. 2 : Comparison of the dispersion of the TO mode propagating along [001] and polarized along [100] for $PuCoGa_5$ and $UCoGa_5$ at 300 K. The solid line is a calculation for $PuCoGa_5$ with $U = 3$ eV and the dashed line is calcultion for $UCoGa_5$ with $U = 0$ eV.

-trons in this compound [6]. The comparison between experimental data and calculation for the lowest TO branch propagating along [001] and polarized along [100] is shown in Fig.2 for the two compounds. The *ab-initio* lattice dynamics calculation shown corresponds to $UCoGa_5$ with $U = 0$ eV and respectively to $PuCoGa_5$ with $U = 3$ eV.

Our study gives new evidence for localized degrees of freedom of f electrons in $PuCoGa_5$ and shows that phonon spectroscopy is an alternate way of probing electronic properties of strongly correlated electron systems. This study is in line with other critical tests of theoretical treatment of 5f electrons, e.g. the one performed on δ-Pu [7].

1 N.J. Curro et al., Nature **434**, 622 (2005).
2 P. Piekarz et al., Phys. Rev. B **72**, 014521 (2005).
3 X. Dai et al., Science **300**, 953 (2003).
4 J.J. Joyce et al., Phys. Rev. Lett. **91**, 176401 (2003).
5 N. Metoki et al., Proceedings of SCES 2005, Vienna.
6 R. Troć et al., Phys. Rev. B **70**, 184443 (2004).
7 J. Wong et al., Science **301**, 1078 (2003).

Electronic Structure Investigations of Pu-Compounds: $PuFeGa_5$, $PuNiGa_5$, $PuFe_{0.5}Co_{0.5}Ga_5$, $PuNi_{0.5}Co_{0.5}Ga_5$ and $PuIn_3$

P.M. Oppeneer[*], S. Lebègue[†], O. Eriksson[*]

[*]Department of Physics, Uppsala University, Box 530, S-754 47 Uppsala, Sweden
[†]Laboratoire de Cristallographie et de Modélisation des Matériaux Minéraux et Biologiques, CNRS-Université Henri Poincaré, B.P. 239, F-54506 Vandoeuvre-lès-Nancy, France

SCIENTIFIC RELEVANCE OF Pu-COMPOUNDS

The interest in Pu-compounds has been revitalized considerably by the discovery[1] of superconductivity at a very high T_c of 18.5 K in the ternary Pu-compound $PuCoGa_5$. The mechanism of the superconducting pair formation has been a point of special attention in the scientific community. It was speculated[1,2] that possibly an *unconventional* pairing mechanism might be responsible for the anomalously high T_c. Several investigations[1,2] showed that $PuCoGa_5$ is close to magnetic ordering, and, consequently, a magnetic mechanism could be responsible for the Cooper pair formation. Recently, two experimental studies[3,4] employing NMR and NQR showed that $PuCoGa_5$ as well as the isoelectronic $PuRhGa_5$ are unconventional, spin-singlet, *d*-wave type superconductors. This type of unconventional order parameter could possibly correspond to pairing mediated by antiferromagnetic spin fluctuations.[3]

In the sequel of the initiating discovery, many actinide compounds, which crystallize in the tetragonal $HoCoGa_5$ structure were synthesized and investigated. An important point–which yet has to be clarified–is what the essential difference is between the two superconducting Pu-115 compounds and other, non-superconducting actinide-115 compounds. Several Pu-based 115-compounds were synthesized, but the only superconducting Pu-compounds so far are $PuCoGa_5$ and $PuRhGa_5$. Moreover, substituting Co by Fe or Ni, its direct, respective neighbours in the Period Table, rapidly quenches the superconductivity.[5] At present it is not understood why the effect of substitution on the Co site is so pronounced. Viewed from the number of electrons in the unit cell, it turns out that superconductivity appears only in a narrow "dome" around the electron filling of 32 valence electrons per unit cell (corresponding to $PuCoGa_5$).

ELECTRONIC STRUCTURE INVESTIGATIONS OF Pu-COMPOUNDS

With the aim to search for differences between the Pu-115 materials, we have performed a computational investigation of the electronic structures of several Pu-115 compounds. We used the density functional theory (DFT) in conjunction with the local spin-density approximation (LSDA) and the generalized-gradient approximation (GGA). The calculations were performed with the full-potential LMTO as well as with the FP-LAPW method, in which scalar-relativistic effects and the spin-orbit interaction are included. In the GGA/LSDA calculations the Pu 5*f* electrons are treated as delocalized valence states. Previously the importance of Coulomb correlations within the Pu 5*f* shell has been pointed out[6,7] for $PuCoGa_5$. To investigate their importance, we also performed LSDA+U calculations for several Pu-115 compounds. The appropriate 5*f* description has to be established through comparison with experiments.

Our GGA calculations show that there exists sensitivity to the band filling (i.e., number of electrons) in these materials. The 3*d*-states of Fe, Co and Ni are mostly retracted from the Fermi energy, although there is in the density of states (DOS) a tail, which extends to several eV above the Fermi level. A part of the Pu 5*f* states is positioned near the Fermi energy.[2,8] To a good approximation, the filling of the 3*d* band leads to a rigid-band-like shift of the Fermi level within the narrow 5*f* band. Because the 5*f* partial DOS is rather steep near the Fermi level, the band filling leads to significant changes of the Fermi surfaces. In particular, the Fermi surface computed for $PuCoGa_5$ is most 2-dimensional, whereas the Fermi surfaces of $PuFeGa_5$ and $PuNiGa_5$ are computed to be more 3-dimensional. This indicates that nesting properties of the Fermi surfaces–which could be important for the pairing interaction–are different for the Pu-115 compounds.

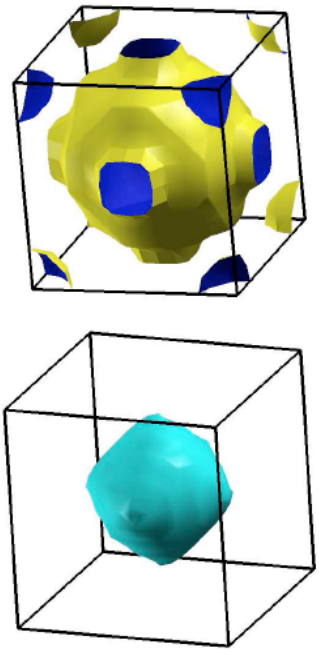

Fig 1: The calculated GGA Fermi surfaces of $PuIn_3$.

RELATED PuGa3 AND PuIn3 COMPOUNDS

Closely related to the Pu-115 compounds are the binary Pu-compounds $PuGa_3$ and $PuIn_3$. An essential building block of the Pu-115's would be the cubic $PuGa_3$ group. However, so far only $PuIn_3$ was synthesized[9] in the cubic $AuCu_3$ phase; it has not been possible to synthesize $PuGa_3$ in the cubic structure. It could be synthesized[10] only in a trigonal and a hexagonal phase, both of which are magnetic. The Fermi surface of $PuIn_3$ was studied[9] recently through de Haas-van Alphen (dHvA) experiments. This study revealed that one part of the Fermi surface of $PuIn_3$ as detected in dHvA experiments, is reasonably described by DFT calculations. We have investigated $PuIn_3$, too, and obtain (in variance with the previous study) one of the Fermi surface sheets to be connected across the zone boundaries (see Fig. 1). Thus, we find overall similar features of the Fermi surface, except for the topology of one Fermi surface sheet. Further de Haas-van Alphen studies would be desirable to achieve a complete picture of the Fermi surface. Also for $PuFeGa_5$ and $PuNiGa_5$ such investigations could be employed to reveal if these materials indeed have a more 3-dimensional Fermi surface.

We gratefully acknowledge fruitful discussions with A.B. Shick, V. Janiš, J.D. Thompson, J.L. Sarrao, N.J. Curro, T. Durakiewicz, J.J. Joyce, E.D. Bauer, G.H. Lander, F. Wastin, J. Rebizant, E. Colineau, P. Boulet, D. Aoki, Y. Haga. K. Kaneko, N. Metoki, R.H. Heffner and Y. Onuki.

1 J.L. Sarrao *et al.*, Nature **420**, 297 (2002).
2 I. Opahle and P.M. Oppeneer, Phys. Rev. Lett. **90**, 157001 (2003).
3 N.J. Curro *et al.*, Nature **434**, 622 (2005).
4 H. Sakai *et al.*, J. Phys. Soc. Jpn. **74**, 1710 (2005).
5 P. Boulet *et al.*, Phys. Rev. B **72**, 104508 (2005).
6 J.J. Joyce *et al.*, Phys. Rev. Lett. **91**, 176401 (2003).
7 A.B. Shick, V. Janiš, and P.M. Oppeneer, Phys. Rev. Lett. **94**, 016401 (2005).
8 T. Maehira, T. Hotta, K. Ueda, and A. Hasegawa, Phys. Rev. Lett. **90**, 157001 (2003).
9 Y. Haga *et al.*, J. Phys. Soc. Jpn. **74**, 2889 (2005).
10 P. Boulet *et al.*, Phys. Rev. B **72**, 064438 (2005).

Fermi Surface, Magnetism and Superconducting Properties of Pu-compounds

Y. Haga[a], D. Aoki[b], H. Yamagami[c], T. D. Matsuda[a], K. Nakajima[d], Y. Arai[d], E. Yamamoto[a], A. Nakamura[a], Y. Homma[b], Y. Shiokawa[b,a] and Y. Onuki [e,a]

[a]Advanced Science Research Center, JAEA, Tokai, Ibaraki 319-1195, Japan
[b]Institute for Materials Research, Tohoku University, Oarai, Ibaraki 319-1313, Japan
[c]Department of Physics, Kyoto Sangyo University, Kyoto 603-8555, Japan
[d]Nuclear Science and Engineering Directorate, JAEA, Tokai, Ibaraki 319-1195, Japan
[e]Graduate School of Science, Osaka University, Toyonaka, Osaka 560-0043, Japan

INTRODUCTION

The discovery of high-temperature superconductivity in plutonium compounds renewed interests in plutonium and other actinide compounds. The high superconducting transition temperature of $PuCoGa_5$ (18.5 K)[1] and $PuRhGa_5$ (8 K)[2] is discussed based on the quasi-two-dimensionality in the electronic state predicted by the 5f-itinerant band calclations[3,4]. On the other hand, there is no experimental work for the investigation of the Fermi surface topology because of the experimental difficulties such as strong radiation damage and self heating effect. It is therefore challenging to clarify the electronic states of plutonium compounds experimentally, by using de Haas-van Alphen Effect (dHvA) or angle-resolved photoemission spectroscopy. In this paper we report the first dHvA study in plutonium compound $PuIn_3$ with the cubic $AuCu_3$ type structure, which can be regarded as a reference compound of $PuCoGa_5$. The result was analyzed based on the itinerant 5f electron picture. Experimental results on magnetic and superconducting properties of $PuRhGa_5$ are also presented.

EXPERIMENTAL

Single crystals of $PuIn_3$ and $PuRhGa_5$ were grown by the flux method using an enriched ^{239}Pu metal as the starting material[5,6]. The sample was characterized by the x-ray diffraction. The single crystal for magnetization and dHvA measurements was encapsulated in a small polyimide tube with typical dimensions ϕ2 x 8 mm. To ensure a good thermal contact between the sample and the cryostat, the sample was mounted on a silver disk. The sample was cooled down using a dilution refrigerator. Because of the self heating effect 5.2 μW of $PuIn_3$, the temperature of the sample is about 10 mK higher than that of the mixture at the base temperature 30 mK. The dHvA effect was measured by the field-modulation technique. The anisotropy of the magnetic susceptibility was measured by the SQUID magnetometer where the field direction was changed by rotating the sample capsule along its axis.

RESULTS[5]

We have succeeded in observing the first dHvA oscillation in plutonium compounds, as shown in Fig. 1. The signal with the dHvA frequency 2.1 x 10^7 Oe shows a clear angular

dependence reflecting the crystal symmetry. The cyclotron effective mass of this branch, determined from the temperature dependence of the dHvA amplitude, is significantly larger than that of an ordinary metal, 4.8 m_0 where m_0 is the electron rest mass. These results show that this signal is attributed to the dHvA oscillation from $PuIn_3$. On the other hand, the signal with a lower frequency 5.5 x 10^6 Oe lacks these features and therefore is considered to come from indium metal. It should also be noted that the dHvA amplitude strongly decreases as function of time, as demonstrated in Fig. 1. Ex 1 was measured 4 days after the crystal growth, while Ex 2 was measured under the same condition 10 days after Ex 1. Such decrease of the dHvA can be attributed to the radiation damage caused by the α-decay of ^{239}Pu. In fact the mean free path of the carrier estimated from the dHvA measurements changes from 860 Å for Ex 1 to 570 Å for Ex 2.

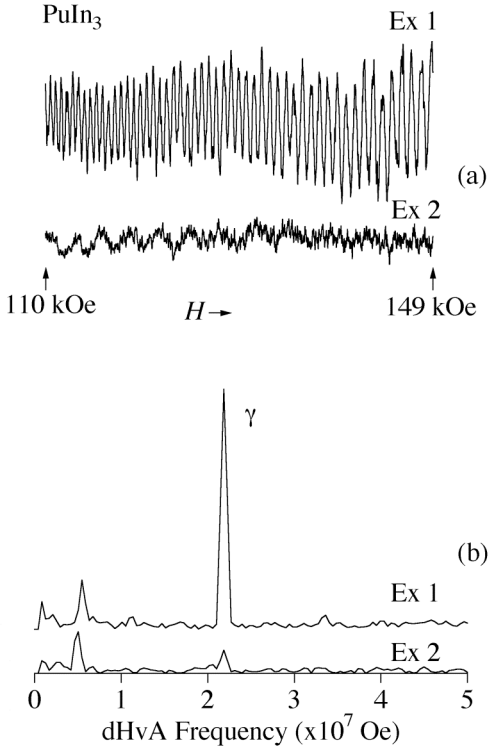

The result of the angular dependence of the dHvA frequency, which corresponds to the extremal cross section of the Fermi surface perpendicular to the field direction, was analyzed by the band calculations. The experimental data agree well with the theory, indicating that the 5f electrons can be treated as itinerant ones. In addition to the dHvA branch detected in the experiment, band calculations predicted 2 more Fermi surfaces which have larger dHvA frequency and cyclotron mass. However, those branches are expected to have significantly small dHvA amplitude and difficult to observe because of the radiation damage as mentioned above.

From the present results, it is expected that the band calculations are valid also for $PuCoGa_5$ and $PuRhGa_5$. The experimental dHvA study for these superconductors are also desired but more challenging because the superconducting mixed state extremely weaken the dHvA amplitude.

1 J. Sarrao *et al*., Nature (London), **420**, 297 (2002).
2 F. Wastin *et al*., J. Phys. Condens. Matter, **15**, S2279 (2003).
3 I. Opahle and P. M. Oppeneer, Phys. Rev. Lett., **90**, 157001 (2003).
4 T. Maehira *et al*., Phys. Rev. Lett. **90**, 207007 (2003).
5 Y. Haga *et al*., J. Phys. Soc. Jpn. **74**, 1698 (2005).
6 Y. Haga *et al*., J. Phys. Soc. Jpn. **74**, 2889 (2005).

What Does $PuCoGa_5$ Teach Us About Pu?

E. D. Bauer[1], J. D. Thompson[1], N. J. Curro[1], T. Durakiewicz[1], J. J. Joyce[1], J. L. Sarrao[1], L. A. Morales[1], J. M. Wills[1], C. H. Booth[2], F. Wastin[3], J. Rebizant[3], J. C. Griveau[3], P. Javorsky[3], P. Boulet[3], E. Colineau[3], G. H. Lander[3]

[1] Los Alamos National Laboratory, Los Alamos, New Mexico 87545, USA
[2]Chemical Sciences Division, Lawrence Berkeley National Laboratory, Berkeley, California 94720, USA
[3]European Commission, Joint Research Centre, Institute for Transuranium Elements, Postfach 2340, 76125 Karlsruhe, Germany

Many of the interesting physical and mechanical properties of plutonium are derived from the behavior of its 5*f* electrons. The existence of six allotropic phases suggest an extreme sensitivity to slight variations in electronic structure, such as the *f*-electron localized to delocalized transition believed to be responsible for the large volume expansion (~25%) when Pu transforms from the α phase to the δ phase. To date, a complete description of the electronic structure of plutonium is still lacking; moreover, the strong electronic correlations that give rise to, among other things, a large Sommerfeld coefficient γ~55 mJ/mol-K^2 and a temperature-independent magnetic susceptibility in the δ phase, cannot be adequately accounted for by theory.

By studying plutonium intermetallic compounds, we may gain unique insight into the nature of Pu itself. The strong electronic correlations in elemental Pu bear a strong resemblance to those found in the $PuCoGa_5$ superconductor [1]. In $PuCoGa_5$, the 5*f* electrons are neither fully localized nor fully itinerant [2]; elements of both kinds of behavior manifest themselves in such properties as an effective moment $\mu_{eff} = 0.7\ \mu_B$, close to that expected for Pu^{3+} (0.84 μ_B) and an enhanced electronic specific heat coefficient $\gamma \sim 100$ mJ/mol-K^2 consistent with moderately heavy fermion behavior [1]. Recent nuclear magnetic resonance measurements [3] provide strong evidence for unconventional *d*-wave superconductivity in $PuCoGa_5$ and for a spin fluctuation energy scale that may not be too different from that of δ-Pu. In addition, a systematic investigation of $ACoGa_5$ (A = U, Np, Pu, Am) reveals 5*f* electron behavior quite similar to the elemental actinides where Pu is poised at the itinerant/localized boundary. In this talk, I will compare the physical properties of $PuCoGa_5$ and elemental Pu and discuss the implications of such a comparison.

[1] J. L. Sarrao et al., Nature **420**, 297 (2002).
[2] J. J. Joyce et al., Phys. Rev. Lett. **91**, 176401 (2003).
[3] N. J. Curro et al., Nature **434**, 622 (2005).

Local Structure, Superconductivity and Radiation Damage in $PuCoGa_5$ and Related Materials

C. H. Booth[*], M. Daniel[*], R. E. Wilson[*], P. G. Allen[†], E. D. Bauer[††], L. Morales[††], J. L. Sarrao[††]

[*]Lawrence Berkeley National Laboratory, Berkeley, California 94708 USA
[†]Lawrence Livermore National Laboratory, Livermore, California 94551 USA
[††]Los Alamos National Laboratory, Los Alamos, New Mexico 87501 USA

In the pure form, the cerium and plutonium based 115 superconductors, such as $CeCoIn_5$ and $PuCoGa_5$, exhibit many interesting properties, not the least of which are their extraordinarily high superconducting transition temperatures (T_c's). The structure of these materials is consistent with a superconducting, two dimensional (2D) Ce-In or Pu-In layer, flanked by non-superconducting layers (see figure). Such an enhancement of T_c in a 2D system furthers the comparisons to the high-T_c copper oxide materials that already bear many significant similarities to rare-earth intermetallics, including relations to magnetic fields and non-Fermi liquid behavior. It is therefore not surprising that there might be a similar dependence on local-structure properties.

We will present x-ray absorption fine-structure (XAFS) data on a variety of 115 materials. We find that the local structure in $CeRh_{1-x}Ir_xIn_5$ is remarkably insensitive to the exact stoichiometry on the transition-metal site,[i] consistent with the slowly varying electronic and magnetic properties ($T_c \rightarrow 0$ K only after ~75% Rh, and even $CeRhIn_5$ is superconducting under applied pressure). On the other hand, substituting Sn for In has a very strong effect, with $T_c \rightarrow 0$ K at only 3.6 mol% Sn. We find that this sensitivity is much stronger than expected given the known superconducting coherence length. XAFS results, however, indicate that the Sn preferentially resides on the in-plane In(1) site[ii], thus concentrating the defects into the superconducting layers and explaining the strong sensitivity to Sn doping. Observed changes in the Kondo temperature will also be discussed in light of these results.

The $PuCoGa_5$ superconductor is not only fascinating as an actinide counterpart to the Ce-based 115's, but also because of its relationship to δ–Pu and the role that the radioactivity of plutonium plays in the structural, electronic and magnetic properties. For instance, this material exhibits local-moment behavior, a property that some have suspected for δ–Pu for many years. We will present Pu L_{III}-edge data that are consistent with this interpretation. Also, these materials exhibit high critical-current densities, probably due to the generation of defects by the radioactive decay of plutonium in the lattice. Our local structure data show a surprisingly large sample volume affected by these decays, suggesting that in addition to the number of Frenkel defects and holes (some estimates are as large as ~3000 pairs per decay), a relatively large sphere exists around each defect that is essentially amorphized. Our ultimate hope is to correlate the observed XAFS amplitude reductions to measurements of such properties as the superconducting coherence length to gain a better understanding of the average distortions in this material, information that would be directly applicable to other plutonium alloys.

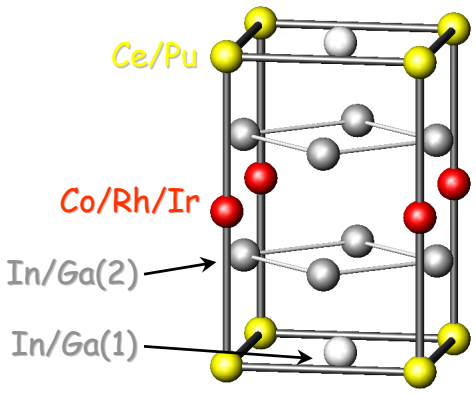

This work was supported by the Director, Office of Science, Office of Basic Energy Sciences (OBES), Chemical Sciences, Geosciences and Biosciences Division, U.S. Department of Energy (DOE) under Contract No. AC03-76SF00098.

[i] M. Daniel, S.-W. Han, C. H. Booth, A. L. Cornelius, P. G. Pagliuso, J. L. Sarrao and J. D. Thompson. Phys. Rev. B, **71**, 054417 (2005).
[ii] M. Daniel, E. D. Bauer, S.-W. Han, C. H. Booth, A. L. Cornelius, P. G. Pagliuso, and J. L. Sarrao. Phys. Rev. Lett. **95**, 016406 (2005).

XAS study of $U_{1-x}Pu_xO_2$ solid solutions

P. Martin[1], G. Carlot[1], M. Ripert[1], S. Grandjean[2], C. Valot[1], P. Blanc[2], C. Henning[3]

[1] CEA Cadarache, DEN/DEC/SESC, bât. 151, 13108 St Paul Lez Durance cedex, France.
[2] CEA Marcoule, DEN/DRCP/SCPS, BP 171, 30270 Bagnols sur cèze cedex, France
[3] Institute of Radiochemistry, Forschungszentrum Rossendorf, P.O. Box 510119, 01314 Dresden, Germany.

The plutonium generated in nuclear power reactors can be re-used at least partially through the exploitation of a Mixed OXide $(U,Pu)O_2$ fuel. Industrially, the manufacture of the MOX fuel proceeds in UO_2 and PuO_2 powders co-crushing, pelletizing and sintering. With this method, a fluorite-type solid solution $(U,Pu)O_2$ is obtained. Currently, rather than a mechanical mixing of pulverulent compounds, a new technique of manufacture for specific needs is under development, based on a co-precipitation of uranium and plutonium (chemical mixture). A better homogeneity of the U and Pu repartition in the solid and at lower temperature is awaited by this 'wet route'. The homogeneity of the final products may represent a significant criterion for an optimized behaviour in power reactors.

The synthesis method was optimized in the CEA Atalante facility at Marcoule [1,2] in order to obtain $(U,Pu)O_2$ solid solutions with a minimal content of synthesis impurities and a O/M ratio equal to 2.0. This method is based on the oxalic co-precipitation of U(IV) and Pu(III) followed by the thermal conversion of the co-precipitate into oxide. Each sample is characterized with X-Ray Diffraction. But, in order to fully investigate the ideality of the solid solution a more local probe is needed. XAFS spectroscopy using synchrotron radiation is an extremely suitable technique to study local atomic and electronic structure of mixed oxides [3,4].

EXPERIMENTAL DETAILS AND RESULTS

A series of solid solutions of $U_{1-x}Pu_xO_2$ (x=0.07, 0.15, 0. 30 and 0.50) were prepared in the ATALANTE Facility. Both UO_2 and PuO_2 reference compounds were synthesized following the same chemical procedure. All the samples were analysed by XRD. In each case, a face centered cubic structure was observed and the cell parameter deducted obeys the Vegard's law.

The XAFS measurements were performed on the ROBL beam line of the European Synchrotron Radiation Facility (Grenoble, France). For each sample, XAS spectra were recorded at both uranium and plutonium L_{III} edges. The evolutions of the Fourier Transform are summarized on the figures 1 and 2. The overall shape of the spectra is almost always the same while the global intensity varies a lot with the plutonium content. Thus, an important decrease of oscillations for the 30 and 15% Pu samples is observed. X-ray diffraction leads to the same result showing a greater disorder than for the PuO_2 and 50 % Pu samples.

At the uranium L_{III} edge, the best fit of the 50% Pu sample leads to the following distances: R_{U-O}=2.352(5) Å, $R_{U-U}=R_{U-Pu}$=3.845(5) Å and R_{U-0}= 4.51(1) Å. The oxygen neighbors are the same as in UO_2 and the U/(U+Pu) ratio is 0.51. The uranium local environment is clearly the one of an

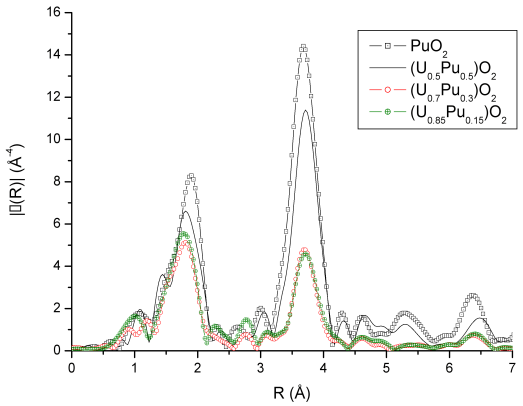

Fig 1: Fourier Transforms of the plutonium L_{III} edge EXAFS.

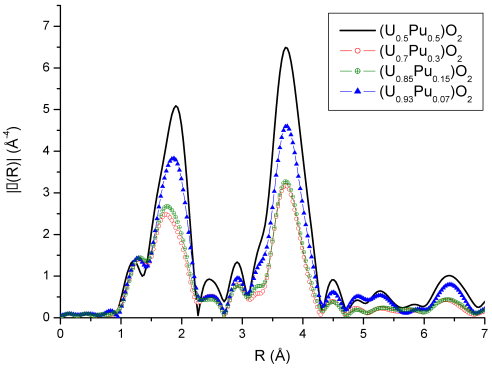

Fig 2: Fourier Transforms of the uranium L_{III} edge EXAFS.

ideal solid solution. The case of plutonium environment is a little more complicated. Indeed, the fitting of the first peak of the Fourier transform of the plutonium L_{III} edge spectra leads to values unsuitable with the fluorite structure. As seen on the figure 1, the shape of this peak (first coordination shell) is no longer gaussian. To fit it, we had to introduce an additional asymmetry term (third cumulant)[7]. Using this method, we finally obtain a shell of 8 oxygen neighbors at a distance of 2.351(5) Å, which is consistent with the result obtained at the uranium edge. Considering the plutonium-metal shell, we also find an ideal solid solution structure with Pu-Pu and Pu-U distances equal to 3.845(5) Å . The Pu/(U+Pu) ratio thus obtained is 47%. The results of the analysis at the two edges clearly show that the chemical procedure used to prepare the $(U_{0.5}Pu_{0.5})O_2$ sample is validated.

For the intermediate plutonium concentrations of 15 and 30%, the local environment of plutonium and uranium is highly perturbed as seen in figures 1 and 2. On the opposite to the 50% plutonium sample, a third cumulant has to be introduced in the fitting procedure even at the uranium edge. Even, if the distances obtained are in good agreement with the Vegard's Law, a doubling of the Debye-Waller ($\sigma^2_{U\text{-}O}$(30% Pu) = 0.014 Å^2 instead of $\sigma^2_{U\text{-}O}$(50% Pu) = 0.0065 Å^2) is observed. This is the signature of a higher disordered structure with a probable hyperstoichiometric composition.

Clearly, as the plutonium content is equal or below 30% at., a great distortion in the Pu local environment is observed. This disorder is incompatible with an ideal solid solution structure. It is interesting to note that EXAFS appears to be the lone technique outlining this discrepancy in plutonium and uranium local environment. Some steps of the process via the wet route checked in this study are currently modified considering their potential influence on the mechanisms of formation of ideal solid solutions, particularly with plutonium content lower than 50%.

[1] S. Grandjean, B. Chapelet-Arab, S. Lemonnier, A-C Robisson, N. Vigier, "Actinides-Basic Science, Applications, and Technology" symposium, MRS Fall Meeting, 26 nov- 2 dec 2005 – Boston, 2005.
[2] S. Grandjean et al, GLOBAL2005, proceeding No. 122, Oct 9-13 2005, Tsukuba, Japan, 2005.
[3] J. Purans, et al, Physica Scripta, T115 (2005) 925-927.
[4] Ph. Martin et al, J. of Nuc. Mat. 312(2003)103-110.
[5] B. Ravel et al, J. Synchrotron Rad. (2005), 12:4, pp. 537-541.
[6] J.J. Rehr et al, Rev. Mod. Phys. (2000) 72, 621-654.
[7] E.A. Stern (1988), Chapter 9, edited by D. C. Koningsberger & R. Prins, New York, John Wiley.

Models and Simulations of Nuclear Fuel Materials Properties

M. Stan, J. C. Ramirez, P. Cristea, B. P. Uberuaga, S. Srivilliputhur, C. Deo, S. Y. Hu, S. P. Rudin, J. M. Wills.

Los Alamos National Laboratory, U. S. A.

INTRODUCTION

In a typical fuel element, cylindrical UO_2 fuel pellets are stacked in a steel cladding. The gap between the cladding and the fuel pellet is filled with helium. The fission reaction generates heat that is diffused mostly outwards in the radial direction. Due to the Soret effect, the gradients in temperature induce oxygen diffusion which in turn triggers the conventional Fickian diffusion. The counterbalancing effects of the Soret and Fickian fluxes are responsible for a variation of oxygen concentration through the fuel pellet even at steady state [1,2]. Conversely, the temperature variation through the pellet is preserved because of the heat generation, which manifests itself as a source term in the heat equation.

To address the complexity of the phenomena that occur in a fuel element, a new multi-scale and multi-physics method was developed at LANL. The method incorporates theory-based atomistic and continuum models into finite element simulations to predict thermo-mechanical properties of alloys and ceramics. By relating micro and nano-scale models to the macroscopic equilibrium and non-equilibrium simulations, the predictive character of the method is improved. The multi-scale approach was applied to calculations of phase stability and defect concentration in PuO_{2-x}, simulations of heat and mass transport in UO_{2+x}, and simulations of irradiation effects in Fe.

MODELS

The concentration of oxygen atoms is often expressed in terms of the non-stoichiometry, x in UO_{2+x}, which is strongly related to the type and concentration of point defects. Following the pattern of a recently published model [3] of PuO_{2-x}, we included in the present model four types of point defects that are considered major contributors to the lattice disorder of UO_{2+x}: U^{5+} uranium ions, Frenkel pairs, oxygen interstitials, and oxygen vacancies. The cation (U) sublattice was treated as ideal, in the sense that the concentrations of uranium vacancies and uranium interstitials were both ignored. At this stage, the Coulomb interaction between the charged species and the spatial correlations due to the exclusion effects was not included. The defect species equilibrium have been described using the general mass action equations, supplemented by charge conservation and lattice geometry constraints. This model was tested against experimental data using a Mathcad code. Given the enthalpies and the entropies of reaction between various types of defects the program predicted the concentration of various point defects and the stoichiometry as functions of temperature and oxygen partial pressure.

SIMULATIONS

We first examined the case fully radial heat conduction and oxygen diffusion, at steady state. The temperature distribution was calculated in the fuel, gap and cladding while the non-stoichiometry was only calculated in the fuel. We use typical dimensions of R_{rod} = 4.3 10^{-3} m and R_{clad} = 4.833 10^{-3} m, and a gap of 0.03 mm. For the temperature in the outer face of the steel cladding, we set Dirichlet boundary conditions by fixing the temperature at 750 K, which represents a typical operating temperature. Similarly, for the outer edge of the fuel rod, we set the non-stoichiometry to 0.001. For the heat generation rate due to the fission reaction, we used a typical [4] value Q = 4.304 10^{8} W/m^{3}.

The temperature and non-stoichiometry distributions along the radial direction of a fuel rod were calculated. The heat generation due to the fission reaction caused the temperature within the rod to be the highest at the center. Since heat is extracted from the outer surface of the cladding, the temperature decreased with increasing radius, as expected. The oxygen atoms re-distributed such that hyperstoichiometry was higher in the hotter regions.

REFERENCES:

1. S. R. De Groot, *Thermodynamics of Irreversible Processes*, North Holland Publ. Co., Amsterdam, 1951.
2. C. Sari and G. Schumacher, J. Nucl. Mater., **61** (1976) 192-202.
3. M. Stan and P. Cristea, J. Nucl. Mater., **344** (2005) 213–218.
4. M. Kazimi, *et al.* “Fission Gas Release Models of Heterogeneous Fuels for Plutonium Burning”, presentation at the MIT Center for Advanced Nuclear Energy Systems.

Abstract of Presentation at International Conference
"Plutonium Future – Science 2006"
(Pacific Grove, California, the USA, July 9-13, 2006)

Development of Fuel Material with Porous Zirconium Carbide Inert Diluent for Plutonium and Minor Actinides Recycling in Fast Reactors

V.K. Orlov, E.M. Glagovsky, G.M. Blukher, A.P. Ivanov, I.A. Shlepov

A.A. Bochvar VNIINM, Moscow, Russia

An effective technique of atomic power nuclear waste treatment resulting in the waste radiotoxicity decrease is the reactor reprocessing technique that ensures the possibility to develop a closed fuel cycle. The technique is based on recycling of plutonium and minor actinides (MA) – neptunium, americium and curium extracted from spent nuclear fuel as a new fuel for fast reactors. This technique is more attractive because it allows generating an additional energy from the produced and stored plutonium and MA. The fuel with an inert diluent without uranium is of a great interest for most effective recycling of MA and plutonium [1,2].

As an option of such fuel, the authors proposed and investigate the composite material, patented at VNIINM, on the basis of zirconium carbide porous skeleton with introduction of plutonium dioxide and minor actinides oxides in the skeleton pores [3]. The skeleton type inert diluent on the basis of porous zirconium carbide has a complex of unique properties – thermalphysic, physical-mechanical, thermodynamic, radiation, high melting temperature ~ 3500 °C, thermal conductivity rising with operating temperature rise, and also chemical, thermodynamic and radiation stability. The positive characteristics of such type of fuel are a comparative simplicity of the fabrication process and its universality. Reactors with this type of fuel should have the negative sodium void reactivity effect (SVRE) that allows introducing a significant amount of MA (up to 30-40 %) in such fuel.

On the basis of calculation, the requirements are identified for characteristics of the fuel composition having the zirconium carbide porous skeleton matrix to use it in the operating fast reactor BN-600. The calculations show that it is possible to transmute 60 kg of Np-237 per year in

the reactor BN-600. Adding Pu-238 generated during transmutation of Np-237 to plutonium fuel in the active core allows making the plutonium unsuitable for weapon purposes, at that, about 200 kg of plutonium per year is burnt up. Subject to these requirements the flowsheet is developed for fabricating the fuel cores with the zirconium carbide porous matrix.

Under the developed flowsheet the cores pilot batches of compositions ZrC-simulator MA (CeO2), ZrC-PuO_2 are fabricated. The cylindrical cores had the diameter of 5.9 mm, the length of 40–70 mm, the compression strength of 11–14 MPa.

The skeleton material had an open porosity of 60–70%. The skeleton material phase composition identified by X-ray diffractometry method (FCC with the period a = 4.691 – 4.700 Å) was consistent with the zirconium carbide stoichiometric composition.

The fissile component content in the core material changed subject to impregnation mode. The cores are fabricated with the fissile component content (CeO_2, PuO_2) over the range from 3.9 up to 38.0%.

The further investigation paths are outlined, which proximate purpose is to fabricate an enlarged batch of fuel cores having the specified composite fuel for testing in the research reactor with subsequent investigations of the irradiated material.

References

1. Bibilashvily J.K., Glagovsky E.M., Bayburin G.G., Shlepov I.A., Blukher G.M., Ivanov A.P., Khandorin G.P. “Development and study of properties of fuel materials having the skeleton type inert diluent (without ^{238}U) for recycling of RG and WG plutonium and minor actinides in fast reactors with an advanced active core”. VNIINM selected works, vol. 1. - 2002. - p.186-188.
2. C. Degueldre. "Inert matrix fuel has the potential to produce electricity while burning up more plutonium." Actinide Research Quarterly. Nuclear Materials Technology/Los Alamos National Laboratory, 1st/2nd quarter 2003, p. p. 23-30.
3. Glagovsky E.M., Bayburin G.G., Blukher G.M. The RF Patent No.2231141. “A composite fuel material and its fabrication technique”. Pubd. June 20, 2004.

Ion beam irradiation of actinide-doped pyrochlores

J. Lian[*], R. C. Ewing[*], L. M. Wang[*], S. V. Yudintsev[†], S. V. Stefanovsky [‡]

[*] University of Michigan, Ann Arbor, MI 48109, USA
[†] Institute of Geology of Ore Deposits RAS, Moscow 109017, Russia
[‡] SIA Radon, Moscow 119121, Russia
Email: rodewing@umich.edu

The safe disposition of fissile Pu from dismantled nuclear weapons and the "minor" actinides (Np, Am, Cm) generated by the nuclear fuel cycle remains a major challenge for the development of next generation nuclear reactors. Recently, there has been extensive interest in using materials with fluorite and fluorite-related structures, such as isometric pyrochlores, as potential host phases for the immobilization of actinides, particularly Pu [1]. Systematic ion irradiation studies of stoichiometric lanthanide pyrochlores ($Ln_2B_2O_7$) (B = Ti, Zr, and Sn) have indicated that the radiation response of the pyrochlore compounds is highly dependent on compositional changes. Both the ionic size and cation electronic configurations (e.g., bond-types) affect the structural distortion from the ideal fluorite structure and thus the response of pyrochlore-structure types to ion beam irradiation [1]. In this study, several actinide-doped pyrochlores were synthesized, including $(Ca_{0.62}Gd_{0.97}U_{0.23})(Zr_{0.84}Ti_{1.34})O_{6.90}$, $(Ca_{0.47}Gd_{0.95}Th_{0.40})(Zr_{1.29}Ti_{0.89})O_{7.05}$, $(Ca_{0.44}GdTh_{0.42})Zr_{2.13}O_{7.05}$, and $Ca_{0.91}Th_{0.84}Zr_{2.25}O_{7.09}$, and their response behaviors upon radiation damage were simulated by 1 MeV Kr^{2+} ion irradiation under in-situ TEM observation. The ion beam irradiations of Ce-doped pyrochlore ($CaCeTi_2O_7$) as well as the solid solution of $(La_{1-x}Ce_x)_2Zr_2O_7$ (x = 0, 0.1, 0.2, 1) were also performed, in which Ce was used as an analogue element for Pu because of their similarities in charge and size.

Figure 1 shows the critical amorphization fluences of actinide-doped pyrochlores irradiated by 1 MeV Kr^{2+} as a function of temperature. The critical amorphization temperatures of $CaCeTi_2O_7$, $(Ca_{0.62}Gd_{0.97}U_{0.23})(Zr_{0.84}Ti_{1.34})O_{6.90}$, and $(Ca_{0.47}Gd_{0.95}Th_{0.40})(Zr_{1.29}Ti_{0.89})O_{7.05}$ are ~1060, 820 and 550 K, respectively. No ion irradiation-induced amorphization has been observed in $(Ca_{0.44}GdTh_{0.42})Zr_{2.13}O_{7.05}$ and $Ca_{0.91}Th_{0.84}Zr_{2.25}O_{7.09}$, subjected to 1 MeV Kr^{2+} at room temperature. The greater radiation "resistance" of actinide-doped pyrochlores, as compared with that of Ce-doped composition, is consistent with the larger average ionic radius at the B-site with increasing concentrations of Zr. In the solid solution binary of $(La_{1-x}Ce_x)_2Zr_2O_7$ (x = 0, 0.1, 0.2, 1), $La_2Zr_2O_7$ can be amorphized by a 1.0 MeV Kr^{2+} ion irradiation at 25 and 293 K at doses of ~1.19 and ~3.55 dpa, respectively, similar to that observed under 1.5 MeV Xe^{+} irradiation [2]. With the addition of Ce in lanthanum-zirconate pyrochlore structure (x = 0.1), no ion irradiation-induced amorphization has been observed at room temperature. The critical amorphization dose for $(La_{0.9}Ce_{0.1})_2Zr_2O_7$ at 25 K is ~3.55 dpa, and with increasing Ce-content, a higher dose (~5.20 dpa) is required to fully amorphize $(La_{0.8}Ce_{0.2})_2Zr_2O_7$ at 25 K. No amorphization occurred for $Ce_2Zr_2O_7$ at 25 K at a dose of ~7 dpa. The addition of Ce into the $La_2Zr_2O_7$ structure increases the radiation stability of materials (Figure 2), which may be attributed to the decreasing average radius of cations in the A-site, resulting from the smaller ionic radii of Ce^{3+} (0.114 nm) and Ce^{4+} (0.097 nm) as compared to La^{3+}(0.116 nm). These results suggest that complex pyrochlore

compositions, caused by the incorporation of actinides and lanthanides, may exhibit dramatic differences in their response to a radiation environment. The addition of actinides may enhance the radiation stability of these materials. Data such as these allow one to design a specific pyrochlore composition with a desirable radiation stability and chemical durability as a potential waste form for the immobilization of actinides, particularly Pu.

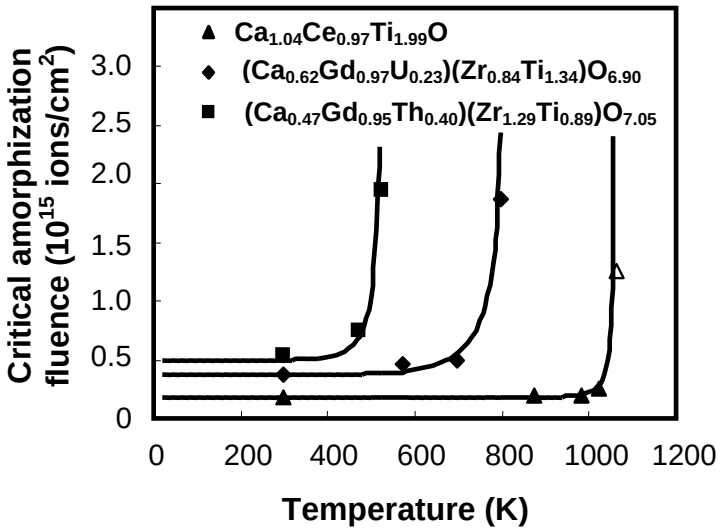

Figure 1. Critical amorphization fluences of actinide-doped pyrochlore vs. irradiation temperature.

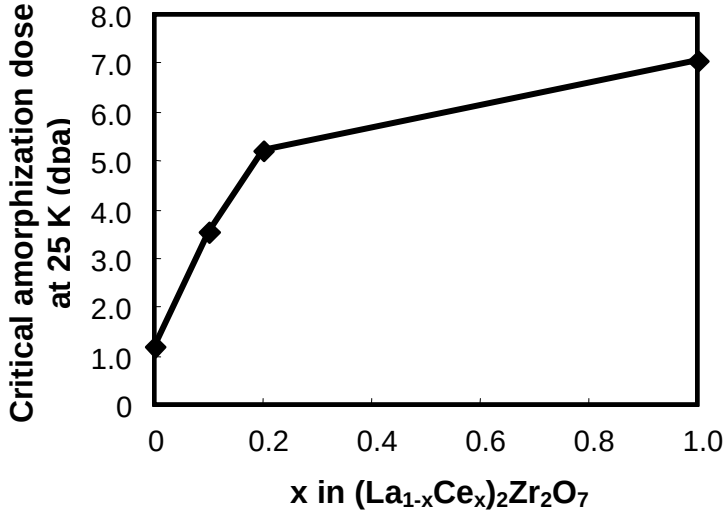

Figure 2. The addition of Ce in the solid solution of $(La_{1-x}Ce_x)_2Zr_2O_7$ enhances the radiation stability.

This work was supported by the Office of Basic Energy Sciences, USDOE under DOE grant DE-FG02-97ER45656.

1. R. C. Ewing, W. J. Weber, and Jie Lian, Journal of Applied Physics 95 (2004) 5949-5971.
2. J. Lian, X. T. Zu, K. V. G. Kutty, J. Chen, L. M. Wang, and R. C. Ewing, Phys. Rev. B 66 (2002) 054108.

High Temperature Reactivity of Mixed Uranium and Plutonium Carbide Fuels with Silicon Carbide as an Inert Matrix. Efficiency of Refractory Metals as Interdiffusion Barriers.

J. Léchelle[1], E. Belval-Haltier[1], R. Belin[1]

[1] CEA, CEN Cadarache, DEN/Cad/DEC/SPUA/LMPC, Bât 717, 13108 Saint-Paul Lez Durance

High Temperature Gas Cooled Fast Reactors for the fourth generation of reactor studies have lead to chemical compatibility studies between the foreseen fuel and matrix materials, in normal operation, incidental and accidental conditions. Reactivity experiments were first carried out for temperature incidental conditions.

A first experiment was carried out at 1650°C - 100h for a sample which consisted of a mixture of mixed uranium and plutonium carbide (14 mole %) and beta-SiC (86 mole %) powders. The temperature was representative of accidental conditions. The aim was to determine whether new liquid phases or new solid phases may appear thus disturbing the reactor core behaviour and in the case it occurs to find a way to dodge this problem by adding a thin barrier material.

The mixed uranium and plutonium carbide comes out of a fabrication made by TUI dedicated to NIMPHE2 irradiation ("NItrure Mixte PHenix"). As shown by XRD powder patterns, it is made of a mixture of three monocarbide phases the lattice parameter of which is 4.979, 5.000 and 5.017 Å as well as a sesqui-carbide phase (8.117 Å). Chemical composition of C, N and O elements can be interpreted by a partial oxidation of an initial mixture of (U,Pu)C to give these three Fm3m phases and $(U,Pu)_2C_3$. Under the assumption of a Vegard's law the mixture would consist of 86 w% of $U_{0.78}Pu_{0.22}C_{0.9}O_{0.1}$ and 14 w% of $(U_{0.65}Pu_{0.35})_2C_3$.
The cubic polymporhic phase (3C) of silicon carbide was used for this study.
Although U-Si-C phase diagram is known, very limited thermodynamic data are available for the description of Pu-Si-C and U-Pu-Si-C phase diagrams hence limiting potential valuable computations on the expected reaction products.
XRD diffraction pattern of the mixture after the experiment shows $U_{0.8}Pu_{0.2}C$ as main phase, beta-SiC at a lower amount, a significant amount of $M_{20}Si_{16}C_3$ where M could be either U or Pu, a less abundant Pu_2C_3 and tetragonal PuC_2 phases, trace amounts of hexagonal beta-$PuSi_2$. Guinet indicates that $U_{20}Si_{16}C_3$ shows a peritectic decomposition at 1600°C.Thus $M_{20}Si_{16}C_3$ may have appeared while cooling down the temperature. This compound shows a slight deviation of its c lattice parameter value (8.012±0.002 Å) from $U_{20}Si_{16}C_3$ value. This high reactivity deters from using these two materials in direct contact one with the other in reactor at this temperature. Studies at a lower temperature (1400°C) are under way .

Mo, Mo-Re, W and $W_{0.95}Re_{0.05}$ have been considered as refractory metal diffusion barriers between (U,Pu)C and SiC.
Under neutron flux W transmutes into Re and might induce a phase change of W-Re in the reactor. Ekman, Persson and Grimwall [1] have shown that under a Re mole fraction equal to

0.3, the CC phase remains stable. Re cluster spreading (after W transmutation) and cluster diffusion should maintain Re concentration under this threshold value. Phase instability is thus unlikely in the case where Re/(W+Re)=5%.
A sandwich material was made of a layer of Mo, a layer of NIMPHE2 mixed carbides and a layer of $W_{0.95}Re_{0.05}$. It underwent a thermal treatment at 1800°C during 6h in a HF oven. This high temperature was chosen in order to enlarge the thickness of the reactivity product layer and facilitate its observation. It was then observed by optical microscopy (Figure 1) and some material was sampled at the interfaces (Mo side of Mo/(U,Pu)C interface, (U,Pu)C side of Mo/(U,Pu)C interface, (U,Pu)C side of (U,Pu)C/W-Re interface and W-Re side of (U,Pu)C/W-Re interface) for an XRD characterization. Only two interface XRD results are yet available: the Mo side of the first interface shows evidence of Mo_2C and $UMoC_2$ phases while the W-Re side of the interface shows evidence of $U_2W_4C_4$ and W_2C phases.

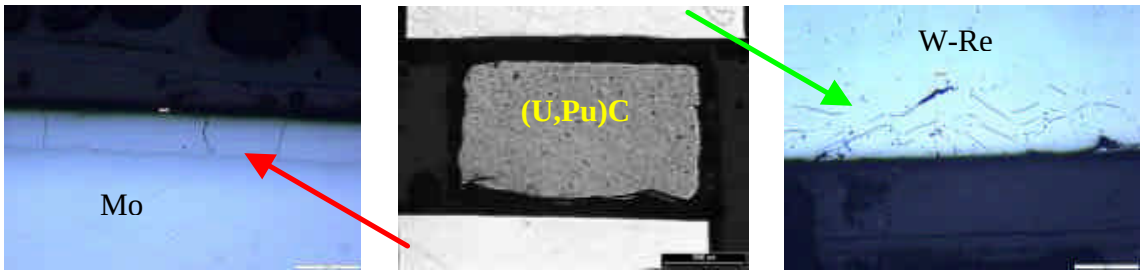

Fig. 1: optical microscopic observations of Mo/(U,Pu)C/W-Re sandwich after thermal treatment.

Mo and W-Re high temperature reactivity with SiC experiments were carried out at 1600°C for 100 hours. 60µm long Si rich fingers were observed by means of a SEM. Local W/Si ratios were measured confirming the possibility of occurrence of W_5Si_3 phase. This is in agreement with studies, reported by several authors [2, 3], which make evidence, between 1700 and 1900°C, of the succession of phases: $SiC/WSi_2/WC/W_5Si_3/W_2C/W$.
At 1600°C, even after 6 hours, a 60µm thick reactivity layer can be observed in Mo in contact with SiC. SEM local analysis of Mo and Si coupled with the measurement of their total weight percent give results compatible with Mo_5Si_3 and Mo_2C phases. These phases were observed with XRD experiments by other authors in the same conditions.

As a conclusion, at 1600°C NIMPHE2 carbide reacts with SiC. A Mo or W-Re diffusion barrier would have the drawback of consuming a part of the (U,Pu)C carbide carbon. To avoid this problem W-Re would have to be coated with Re on one of its sides in order to limit its reactivity with (U,Pu)C. The other side of W-Re would need to be protected by another material in order to limit its reactivity with SiC.

[1] Ekman, Persson and Grimwall, J. Nuc. Mat. 278 (2000) 273-276
[2] S.J. Son, T. Hinoki, A. Kohyama, in proceedings of ICAPP'05, Seoul, Korea, 15-19 May 2005, paper 5506, Interfacial properties and phase behaviour of W coated on SiC and SiC/SiC composites for advanced Nuclear Energy Systems
[3] B.V. Cockeram, BETTIS Atomic Power Laboratory, US DOE contract #DE-AC11-98PN38206, B-T-3255, November 1999, The diffusion bonding of Silicon carbide and boron carbide using refractory metals

Weapons-Grade MOX Fuel Burnup Characteristics in Advanced Test Reactor Irradiation

Gray S. Chang

Idaho National Laboratory
P. O. Box 1625
Idaho Falls, ID 83415-3885
e-mail: gray.chang@inl.gov

ABSTRACT

Mixed oxide (MOX) test capsules prepared with weapons-derived plutonium have been irradiated to a burnup of 50 GWd/t. The MOX fuel was fabricated at Los Alamos National Laboratory by a master-mix process and has been irradiated in the Advanced Test Reactor (ATR) at the Idaho National Laboratory (INL). Previous withdrawals of the same fuel have occurred at 9, 21, 30, 40, and 50 GWd/t[1, 2, 3, 4]. Oak Ridge National Laboratory (ORNL) manages this test series for the Department of Energy's Fissile Materials Disposition Program (FMDP).

A UNIX BASH (Bourne Again SHell) script CMO has been written and validated at the Idaho National Laboratory (INL) to couple the Monte Carlo transport code MCNP[5] with the depletion and buildup code ORIGEN-2[6] (CMO). The new Monte Carlo burnup analysis methodology in this paper consists of MCNP coupling through CMO with ORIGEN-2, and is therefore called the MCWO[7, 8]. MCWO is a fully automated tool that links the Monte Carlo transport code MCNP with the radioactive decay and burnup code ORIGEN-2.

The fuel burnup analyses presented in this study were performed using MCWO. MCWO analysis yields time-dependent and neutron-spectrum-dependent minor actinide and Pu concentrations for the ATR small I-irradiation test position. The purpose of this report is to validate both the Weapons-Grade Mixed Oxide (WG-MOX) test assembly model and the new fuel burnup analysis methodology by comparing the computed results against the neutron monitor measurements and the irradiated WG-MOX post irradiation examination (PIE) data.

References:

1. R. N. Morris, C. A. Baldwin, B. S. Cowell, S. A. Hodge, et. al. “MOX Average Power Early PIE: 8 GWd/MT Final Report,” Oak Ridge National Laboratory, ORNL/MD/LTR-172, November 1999.

2 R.N. Morris, C. A. Baldwin, S. A. Hodge, L. J. Ott, C. M. Malone, N. H. Packan, “MOX Average Power Intermediate PIE: 21 GWd/MT Final Report,” Oak Ridge National Laboratory, ORNL/MD/LTR-199, December 2000.

3. R.N. MorriS, C. A. Baldwin, S. A. Hodge, N. H. PACKAN, “MOX Average Power 30 GWd/MT PIE: Final Report,” Oak Ridge National Laboratory, ORNL/MD/LTR-212, November 2001.

4. R. N. Morris, C. A. Baldwin, S. A. Hodge, N. H. Packan, “MOX Average Power 40 GWd/MT PIE: Final Report,” Oak Ridge National Laboratory, ORNL/MD/LTR-241, Volume 1, August 2003.

5. J. Briesmeister (Editor), ‘MCNP—A General Monte Carlo N-Particle Transport Code, Version 4C,’ LA-13709-M, Los Alamos National Laboratory (2000).

6. A. G. Croff, “ORIGEN2: A Versatile Computer Code for Calculating the Nuclide Compositions and Characteristics of Nuclear Materials,” Nuclear Technology, Vol. 62, pp. 335-352, 1983.

7. G. S. Chang and J. M. Ryskamp, "Depletion Analysis of Mixed Oxide Fuel Pins in Light Water Reactors and the Advanced Test Reactor," Nucl. Technol., Vol. 129, No. 3, p. 326-337 (2000).

8. G. S. Chang, " V&V of A MONTE CARLO BURNUP ANALYSIS METHOD - MCWO," Idaho National Engineering and Environmental Laboratory (INEEL) external release report, to be published in May, 2005.

Inductive Cold Crucible Melting of Actinide-Doped Murataite-Based Ceramics

Stefanovsky[*], S.V., Ptashkin[*], A.G., Knyazev[*], O.A., Dmitriev[*], S.A.
Yudintsev[+], S.V., Nikonov[+], B.S.
*SIA Radon, 7th Rostovskii lane 2/14, Moscow 119121 RUSSIA
[+]Institute of Geology of Ore Deposits RAS, Staromonetny lane 35, Moscow 119017 RUSSIA

Introduction

An inductive cold crucible melting (ICCM) is an effective method for growing of single crystals for various technical and jewelry purposes and production of glassy and ceramic materials.[1] The ICCM is currently developed as an alternative to vitrification of high- (HLW)[2,3] and intermediate-level wastes (ILW)[4] in Joule-heated ceramic melters. The ICCM seems to be very effective method of HLW ceramization due to small dimensions, high-active hydrodynamic regime, and high temperature availability. This method was used to producing numerous ceramic waste forms (see, for example[5-8]).

Murataite-based ceramics are considered as perspective matrices for complex actinide/rare earth-bearing wastes[9] due to high chemical durability[10] and capability of the murataite structure to accommodating elements with widely variable ionic sizes and radii.[9,11,12] Therefore, it is expedient to apply the ICCM to develop high-productive, compact, and remote operable process with high volume reduction yielding leach resistant waste form.

Results

Specified chemical compositions of the ceramic were as follows (wt.%): 5 Al_2O_3, 10 CaO, 55 TiO_2, 10 MnO, 5 Fe_2O_3, 5 ZrO_2, 10 AnO_2 (An = U, Th). The UO_2-doped ceramic (U-ICCM) was produced at the Radon bench-scale cold crucible (108 mm in inner diameter, stainless steel) unit energized from a 1.76 MHz/60 kW generator. The ThO_2-doped ceramic (Th-ICCM) was produced in a lab-scale unit with a 65 mm inner diameter copper cold crucible energized from a 5.28 MHz/10 kW generator.

At the U-ICCM ceramic production starting melt formation using a SiC rod took 22 min followed by batch feeding in portions for 15 min, homogenization for 5 min and pouring into container. Totally batch in amount of 5 kg was fed and product in amount of ~2.7 kg was poured into container (about 2.3 kg remained as “dead volume” in the crucible). Because 2.7 kg of ceramic was produced for 20 min, average productivity is 8.1 kg/h or specific productivity – 900 kg/(m^2 h).

The Th-ICCM ceramic was produced in the lab-scale crucible in amount of ~1 kg. Both the ceramics were composed of predominant target murataite-type phases and minor extra phases: rutile, crichtonite and glass (due to melt contamination with Si from the SiC rod) in the U-ICCM ceramic, and crichtonite and traces of thorianite, pyrochlore, and low-symmetry phase in the Th-ICCM ceramic (Figure 1, a,b).

In the U-ICCM ceramic the murataite is represented by three different polytypes with five- (5×), eight- (8×), and three-fold (3×) elementary fluorite unit cell (Figure 1,c-e) composing centre, intermediate part, and rim of the murataite grains, respectively (Figure 1, a,b). Their formulae calculated from the EDS data and suggestion on formation of the murataites structure from pyrochlore and murataite-3 modules[12] are as follows: $Ca_{2.54}Mn_{1.54}U_{0.56}Zr_{0.88}Ti_{7.80}Fe_{0.81}Al_{0.87}O_{27-x}$ (5×), $Ca_{4.33}Mn_{2.99}U_{0.86}Zr_{1.10}Ti_{13.51}Fe_{1.42}Al_{1.78}O_{47-x}$

(8×), and $Ca_{1.37}Mn_{1.37}U_{0.16}Zr_{0.20}Ti_{5.45}Fe_{0.95}Al_{1.50})O_{20-x}$ (3×). Maximum UO_2 content (12.1%) was found to be in the core of grains (5× polytype). UO_2 content in the rim is much lower (5.2%). In the Th-ICCM ceramic the only 5× polytype ($Ca_{2.13}Mn_{1.90}Zr_{0.82}Th_{0.55}Fe_{0.78}Ti_{7.86}Al_{0.96}O_{27-x}$) has been found and Th distribution in the grains is uniform.

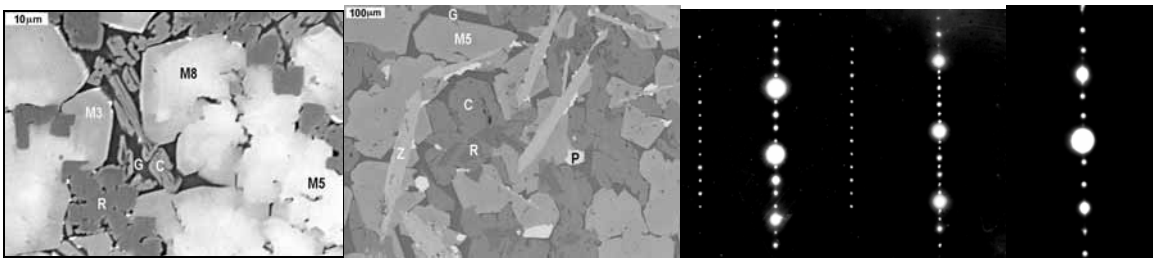

a b c d e

Figure 1. SEM-images of the ceramics U-ICCM (a), Th-ICCM (b) and SAED patterns from (100) plane of inverse lattice of the murataite polytypes 5× (c), 8× (d), and 3× (e).

Discussion

The ICCM is very high-productive process for actinide-waste forms fabrication. Application of a larger-scale (108 mm in diameter) cold crucible provides for low melt cooling rate in both crucible and filled container with sequential crystallization of various murataite polytypes. This yields dense ceramic with zoned structure of the grains with maximum actinide concentration in the core and minimum - in the rim thus reducing their leachability. Melt cooling rate in small cold crucible is higher and fast crystallization resulted in the only (5×) murataite polytype formation with uniform distribution of waste elements. Thus, application of large-scale cold crucibles is a perspective route to development of industrial-scale process and technology for ceramization of actinide-bearing HLW such as actinide or actinide/rare earth fraction of HLW and Am/Cm waste from conversion of excess weapons plutonium to MOX fuel.

References

1) Kuz'minov, Yu.S., Osiko, V.V., Fianites (Russ.), Nauka, Moscow, 2001.
2) Do Quang, R, Petitjean, V., Hollebecque, F., et al., Proc. Waste Management '03 Conf., Tucson, AZ, 2003. CD-ROM.
3) Kobelev, A.P. Stefanovsky, S.V. Knyazev, O.A. et al., The 107th Annual Meeting of The American Ceramic Society, Baltimore, MD, April 10-13, 2005. CD-ROM.
4) Sobolev, I.A., Dmitriev, S.A., Lifanov, F.A., et al., Glass Technol. 46 (1) 28-35 (2005).
5) Vlasov, V.I., Kedrovsky, O.L., Nikiforov, A.S., et al., Back End of the Nuclear Fuel Cycle: Strategies and Options, Vienna, IAEA, 109-117 (1987).
6) Sobolev, I.A., Stefanovsky, S.V., Ioudintsev, S.V., et al., Mat. Res. Soc. Symp. Proc. 465, 363-370 (1997).
7) Day, R.A., Ferenczy, J., Drabarek, E., et al., Proc. Waste Management '03 Conf., Tucson, AZ, 2003. CD-ROM.
8) Stefanovsky, S.V., Kirjanova, O.I., Yudintsev, S.V., Knyazev, O.A. Proc. Waste Management '01 Conf., Tucson, AZ, 2001. CD-ROM.
9) Stefanovsky, S.V., Yudintsev, S.V., Gieré, R., Lumpkin, G.R., in: Energy, Waste, and the Environment: a Geological Perspective, Gieré, R. and Stille, P. (eds) Geological Society, London, 236, 37-63 (2004).
10) Stefanovsky, S.V., Yudintsev, S.V., Perevalov, S.A., et al., Plutonium Futures – The Science – 2006. This volume.
11) Ercit, T.S., Hawthorne, F.C., Canad. Miner. 33, 1223-1229 (1995).
12) Urusov, V.S., Organova N.I., Karimova, O.V., et al., Trans. (Doklady) Russ. Acad. Sci./Earth Sci. Sec., 401, 319-325 (2005).

Phase Transformations in Pu-Al and Pu- Ga Alloys. Effects of Pressure and Temperature on the Kinetics of the Delta-Phase Decomposition

L.F. Timofeeva

A.A.Bochvar VNIINM (All-Russian Research Institute of Inorganic Materials), Moscow, Russia

EVOLUTION OF PHASE DIAGRAMS UNDER PRESSURE

The binary phase diagram at atmospheric pressure as a section of the pressure–temperature - composition PTC diagram results from a regular variation of phase areas with space. PT diagram for Pu and earlier experimental data [1,2,3] underlie schematic phase diagrams for the Pu-Al and Pu- Ga systems over the 0 ~3 GPa pressure range (see Figure 1). As Pu phases disappear with increasing pressure, the binary phase diagram varies from complex one at atmospheric pressure to rather simple at high pressures (see Figure 1). Features of PT binary Pu-Ga (Al) diagrams was analyzed at the pressure of triple points on PT phase diagram for Pu. Our notions on the phase diagrams evolution under pressure were used for experimental constructing of phase diagrams at different pressures.

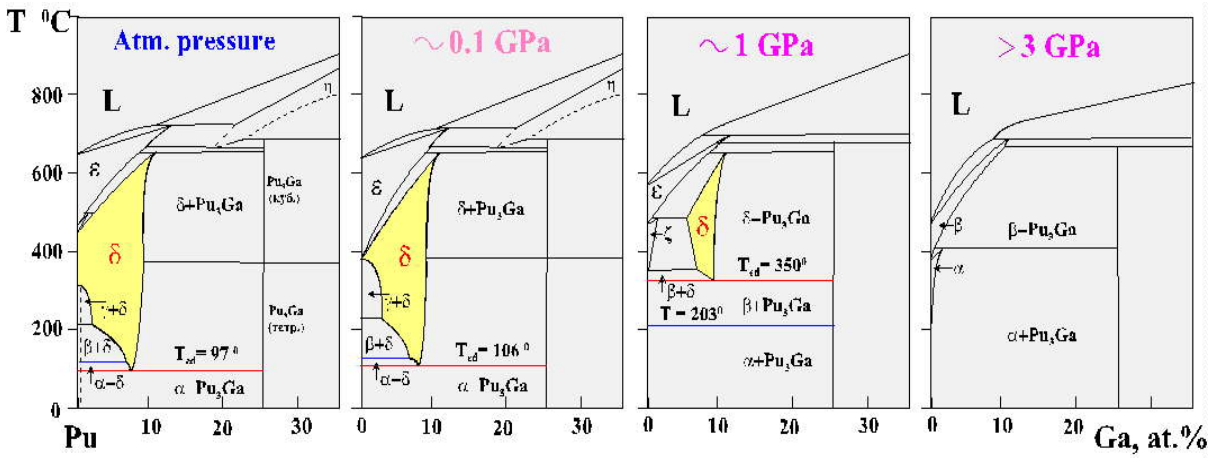

Fig1: Evolution of Pu-Ga Diagram under Pressure (scheme on a base of Experiment and Prognosis)

EXPERIMENTALLY AND THERMODYNAMICALLY DETERMINED δ-PHASE BOUNDARIES

Based on isothermal annealing results under static pressures as large as 0.6-0.8 GPa, δ-phase boundaries for the Pu-Al and Pu-Ga systems were delineated. The thermodynamic calculation of the displacement of the δ-phase boundaries to P ≅ 2-3 GPa correlates well with the experiment. The δ-phase boundary shifts to higher concentrations of Al or Ga on the Pu-side and slightly to Pu on the intermetallic compound side. The δ-region decreases to the point of disappearance. The δ-phase eutectoid decomposition temperature at different pressures was evaluated from intersection of boundaries on the $N_{моль}^{Al(Ga)}$- 1/T K coordinates. The eutectoid decomposition temperature (T_{ed}) versus pressure was plotted (see Figure 2). Parameters of the four-phase equilibrium (δ,α,β, Pu_3Ga) at point "H" on PT binary PuGa diagram were determined. Point "H" is a projection on the PT plane of the HH line. It is line of intersection of two three-phase equilibrium surfaces on the PTC phase diagram (see Figure 3). Above and below point H the δ-eutectoid decomposition results in βPu + Pu_3Ga and αPu + Pu_3Ga, respectively.

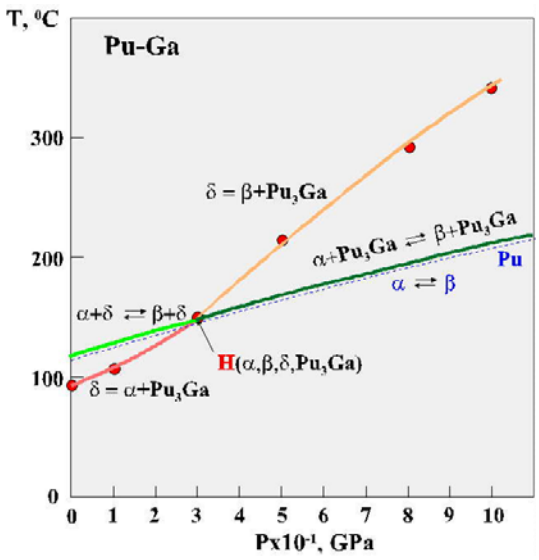

Fig 2: Effect of static pressure P on T_{ed} of PuGa alloys and $T_{\alpha\rightarrow\beta}$ Pu

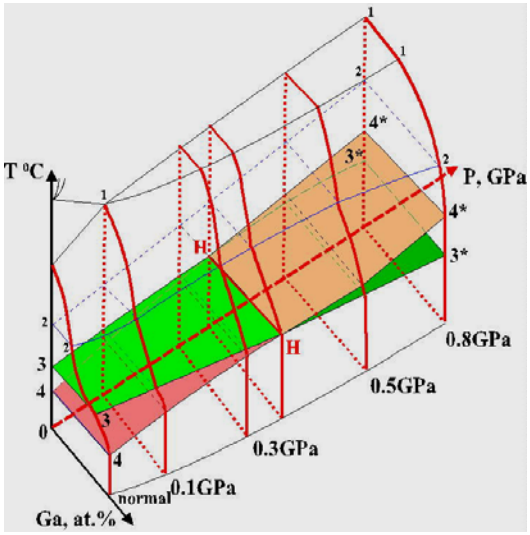

Fig 3: PTC diagram of PuGa- equilibrium 33HH-α+δ↔β+δ; HH3*3*-α+Pu_3Ga↔β+Pu_3Ga; 44HH -δ↔α+ Pu_3Ga; HH4*4*-δ↔β+ Pu_3Ga

KINETICS OF δ-PHASE EUTECTOID DECOMPOSITION

As pressure and temperature increase, the rate of the δ-phase diffusion decomposition rises, the kinetics changes and the latent reaction period decreases from hundreds of hours to a few minutes as opposed to atmospheric pressure. The activation energy established for Pu-Al alloys by two methods, namely, the Avrami equation and the isothermal cross-section method, reduces from 30 kcal/mole at 0,1 GPa to 8 kcal/mole at 0,6 GPa. At a relatively low pressure, the both alloy systems show an eutectoid decomposition of different morphology: laminar for Pu-Ga (see Figure 4) and skeleton-like spheroidized for Pu-Al[2].

With due regard for decomposition acceleration and lower activation energy with increasing pressure, it can be suggested that the eutectoid decomposition can experience shock wave loading in a narrow pressure range.

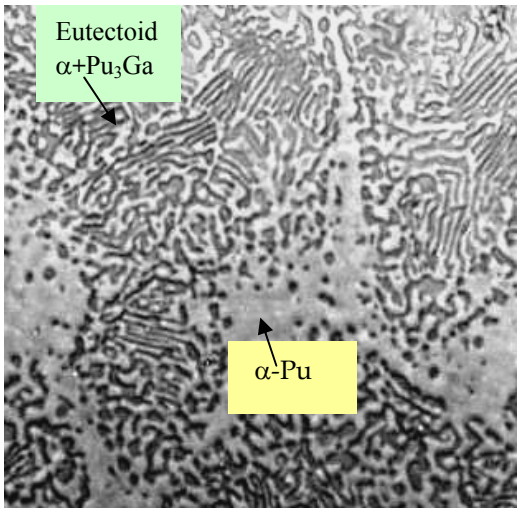

Fig 4: Microstructure of hypoeutectoid Pu-Ga alloy, P≥1 GPa

SUMMARY

Theoretical, experimental and thermodynamically calculated phase diagrams plotted for binary Pu-Al and Pu-Ga systems made it possible to clarify evolution of the phase regions under a pressure up to 2-3 GPa, to establish the temperature and pressure dependence of the eutectoid decomposition temperature With increasing pressure, the δ-phase diffusion decomposition was shown to accelerate and the eutectoid decomposition to transform at relatively low pressures, resulting in an decrease in the activation energy.

1 N.T.Chebotarev, V.S.Kurilo,L.F.Timofeeva, M.A. Andrianov, V.V.Sipin .VANT(rus), seria: Materialovedenie. **37**, (1990).
2 L.F. Timofeeva, *in*: Ageing Studies and Lifetime Extension of Materials, ed. L. Mallinson, N-Y: Kluwer Academic /Plenum, (2001).
3 L.F. Timofeeva. Metallovedenie i termicheskaya obrabotka (rus). **11,** (2004).

Lattice Vibrations in α-Uranium: Non-Linearity and Localization

M. E. Manley,[1,2] M. Yethiraj,[3] H. Sinn,[4] H. M. Volz,[1] A. Alatas,[4] J. C. Lashley,[1] W. L. Hults,[1] G. H. Lander,[5] J. L. Smith[1]

[1]Los Alamos National Laboratory, Los Alamos, New Mexico 87545
[2]Department of Chemical Engineering and Materials Science, University of California, Davis, California 95616
[3]Oak Ridge National Laboratory, Oak Ridge, Tennessee 37831
[4]Argonne National Laboratory, Argonne, Illinois 60439
[5]European Commission, JRC, Institute for Transuranium Elements, Postfach 2340, D-76125 Karlsruhe, Germany

Non-linearity refers to a situation where small perturbations cause large shifts in the excitation spectrum. By this definition the phonons in α-uranium are quite non-linear, the phonon DOS can soften by as much as 10% when the temperature changes by as little as 100 K [1]. Although thermal softening is an expected consequence of anharmonicity, α-uranium is unusual in that it does not show behavior typically associated with a strongly anharmonic solid. First, the elastic energy of expansion can only account for about 10% of the observed softening [1]. Second, the power-spectrum derived energy exhibits linear scaling with temperature, behavior consistent with classical harmonic vibrations [1]. Finally, the features in the phonon DOS sharpen with increasing temperature, the opposite of what is expected from anharmonic lifetime broadening. Based on these observations it has been concluded that the phonon softening in uranium originates with intrinsic temperature dependence in the inter-atomic forces. By extension it has been argued that the softening originates with thermal-changes in the electronic structure [1].

The nature of the non-linearity in the lattice dynamics of α-uranium is clearly unconventional; the usual effects associated with phonon softening are not observed. There is, however, another way non-linearity might appear. Calculations have shown that non-linear dynamics can lead to the formation of spatially localized vibrations [2].

Recent measurements using both inelastic x-ray scattering (IXS) and inelastic neutron scattering (INS) have revealed that at least some of the phonon softening in α-uranium is associated with a new mode forming [3]. Figure 1 shows how the new 14.3 meV mode appears at high temperatures at a ***Q***-position on the [01ζ] zone boundary. Also appearing in Figure 1, a phonon branch that sits just below the new mode energy softens with its formation. A more detailed view of the dispersion curves (not shown here) indicates that other branches also soften, but mainly along the zone boundary [3], and also that intensity is lost in the [00ζ] longitudinal optic phonon branch [3].

Reference [3] provides detailed arguments supporting the hypothesis that the new mode shown in Figure 1 is an intrinsically localized vibration [2]. Briefly, the five main points are:

(1) Extra modes form without a long-range crystal structure change, indicating that the required symmetry breaking must be local;

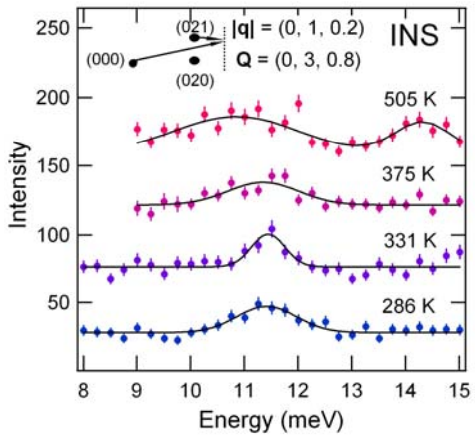

Figure 2: Data showing a new mode emerge near 14 meV at high temperature, together with the softening of the mode at about 11 meV. Data are offset for clarity. The scattering vector, ***Q***, is in the **b-c** plane. The phonon wave vector, ***q***, is at a zone boundary. Data was collected using the at the HFIR facility of Oak Ridge National Laboratory [2].

(2) New modes appear confined to a zone boundary, implying that its spatial periodicity does not extend much beyond the lattice spacing;

(3) Movements of defects involved in plastic deformation are impeded by the new modes while the long-range elastic moduli are not affected;

(4) The mode forms in the presence of a strong non-linearity in the dynamical behavior;

(5) An excess in the heat capacity is found to be consistent with the configurational entropy of having randomly distributed intrinsically localized modes on the lattice.

Interestingly many of the effects of the local mode resemble the effects of adding impurities; a reduction in mechanical ductility and the appearance of mixing entropy [2]. This is because, much like impurities, local modes are distinguishable within the crystal and they have associated strain fields. In other ways the new mode is like a vacancy, since they are thermally activated and occur randomly throughout the lattice.

Inelastic neutron and x-ray scattering measurements are revealing a surprising assortment of exotic dynamical phenomena in uranium, forcing us to rethink our basic understanding of phonon physics as well as a number of related problems including thermodynamic stability and mechanical deformation. It is likely that similar effects are also present in plutonium and other actinides and that future work will prove to be a rich area for advancing our basic understanding of condensed matter physics.

REFERENCES

[1] M. E. Manley, B. Fultz, R. J. McQueeney, C. M. Brown, W. L. Hults, J. L. Smith, D. J. Thoma, R. Osborn, J. L. Robertson, Phys. Rev. Lett. **86**, 3076 (2001).

[2] D. K. Campbell, S. Flach, Y. S. Kivshar, Phys. Today **57**, 43 (2004).

[3] M. E. Manley, M. Yethiraj, H. Sinn, H. M. Volz, A. Alatas, J. C. Lashley, W. L. Hults, G. H. Lander, and J. L. Smith, Phys. Rev. Lett. in press.

Temperature and time-dependence of the elastic moduli of Pu and Pu-Ga alloys

Albert Migliori, D. Miller, D. Dooley, M. Ramos, R.J. Byars, J.B. Betts, I Mihut*

*Los Alamos National Laboratory, Los Alamos, New Mexico 87545

INTRODUCTION

We measured the elastic moduli of Pu and Pu-Ga alloys with three goals. They are 1) Provide accurate elastic moduli, 2) provide accurate temperature dependence, and 3)Measure the relative changes with time. We summarize here results for the time dependences with conclusions and results important to LANL and LLNL programs.

Fig. 1shows an example of an RUS system for use with Pu and Pu-Ga alloys. A complete description of this system and a review of RUS are described by Migliori et al.[1] We have measured Pu, Pu-Ga alloys and an Accelerated-Aging Program (AAP) alloy at ambient and cryogenic temperatures. The AAP alloy "ages" at a rate 16.5 times that of normal ^{239}Pu and it was "made" on 15 May 2002. All measurements presented were performed on fine-grained polycrystal, accurately-polished RPR's of known composition. It is expected that some formation of mechanically-induced alpha-Pu has occurred in delta-Pu specimens, but because all samples are at least as large as a 2mm cube, minimal errors in absolute moduli are calculated from this effect.

TIME DEPENDENCE OF ELASTIC MODULI OF PU AND PU-GA ALLOYS

To understand the variation of the elastic moduli with time in Pu one must keep in mind several effects. These are: 1) Pu-Ga alloys are not thermodynamically stable at ambient temperature. 2) As ^{239}Pu decays radioactively, interstitial-dislocation pairs are produced, about 2200/decay. 3) Decay products include He and metals that are not Pu, and so can change physical properties. A few key referents include: 1) from radioactive decay, $3.16\text{x}10^{-9}$ of the Pu atoms present in a specimen decay per hour, 2) $6.9\text{x}10^{-6}$ Frenkel pairs/hour/atom are produced, 3) From measurements of 3.3 at. % Ga and the 3.9 at. % Ga samples, the maximum long term fractional rate of change of the bulk modulus is of order $9\text{x}10^{-7}$/h, 4) The elastic moduli change at a rate much higher than that of e.g. the density or Frenkel pair retention rate. Thus from the raw Frenkel pair production rate, we can estimate that the elastic moduli change at a fractional rate of order $7\text{x}10^{-5}$/h. These rates are limiting associated with radioactive decay and very low temperature . Any rate substantially different from these must be associated with other physical effects.

It is important to note that the effects seen are much smaller than the error bars for measurements presented above. This is because the precision of RUS for Pu specimens is of order 5 parts in 10^7, but absolute accuracy is limited by errors in the measured size of specimens, of order several tenths of a percent.

Measurements were made using a very-high-precision temperature control system that held temperatures to within a few mK over many days. Good temperature control is crucial because of the strong temperature dependence of the elastic moduli of all samples.

In Fig. 2 we show the time dependence of the moduli of alpha Pu and Pu 2.36 at. % Ga. We can extract an important time scale from these measurements. Note that at 10K where Frenkel pairs are expected, from other studies, to be approximately fully retained, with less than a few tens of percent immediately annealing out, we find that delta Pu shear modulus *decreases* at a fractional

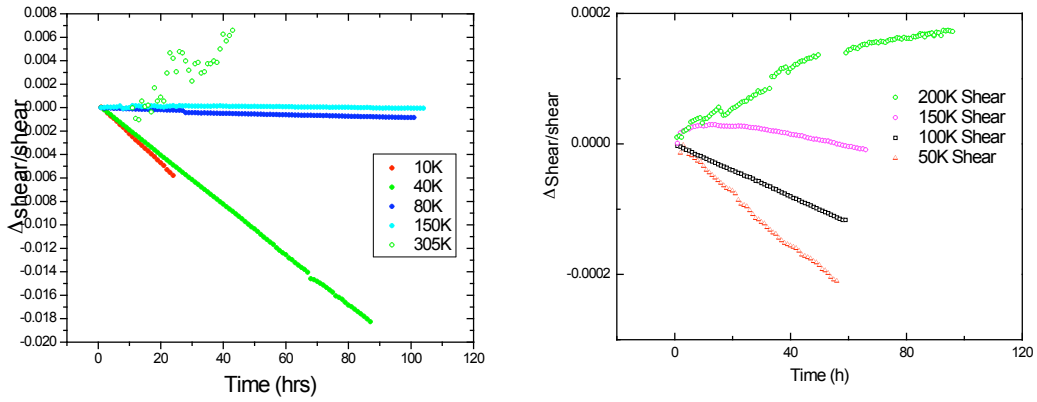

Figure 2. Left: The normalized shear modulus change for alpha Pu versus time and temperature. Right: The normalized shear modulus change for Pu 2.36 at. % Ga versus time and temperature.

rate of about 4×10^{-5}/h and that the modulus of alpha Pu decreases at a higher rate, about 20×10^{-5}/h. The differences are not surprising in light of the differing responses of alpha and delta Pu to radiation damage. *We conclude unambiguously that radiation damage reduces the elastic moduli of Pu alloys.* Thus the time variation of these samples is strictly associated with Frenkel pair production, and *because both alpha and delta change approximately similarly, we can rule out any effects from thermodynamic reversion of the phases predicted by the Russian phase diagram*.

The time scales associated with thermal equilibration of Frenkel pairs can now be determined. Using a relaxation model, our measured difference in bulk modulus of normal and AAP Pu (about 52.3-51.3=2%), the difference in the rate of Frenkel pair production between AAP and normal Pu (a factor of 16) and, and the approximate measured rates of change near room temperature convoluted with the maximum estimated total change ($\tau\ B_0/B_{aging}$=15 years), we can self-consistently find the Frenkel pair main relaxation rate from

$$B = B_0 + B_{aging} e^{\frac{-t}{\tau}}$$

Where we find B_{aging}=0.16%, and τ=8 days. Thus in of order a month, the elastic moduli stabilize, and any further time dependences must be associated primarily with He and U production.

ACKNOWLEDGEMENTS

This work was supported byt the State of Florida, the NNSA, and the LANL laboratory directed research and development program and Enhnanced Surveillance.

The unique high-pressure behaviour of curium probed further using alloys

S. Heathman[1], R. G. Haire[2] T. LeBihan[3], R. Ahuja[4], S. Li[5], W. Luo[4] and B. Johansson[4, 6]

[1.] European Commission, JRC, ITU, Postfach 2340, D-76125, Karlsruhe, Germany
[2] Oak Ridge National Laboratory, PO 2008, Oak Ridge, TN, USA 38831-6375
[3] CEA-Centre de Valduc, F-21120 Is-sur-Tille, France
[4] Dept. of Physics, Uppsala University, Box 530, S-751 21 Uppsala, Sweden
[5] Dept. of Physics, Virginia Commonwealth University, Richland, VA 23284
[6] Royal Institute of Technology, Brinellvägen 23, SE-10044 Stockholm, Sweden

INTRODUCTION

The role of the 5f electrons in the actinide series has been of prime interest for many years. The abrupt changes in volume and structural behaviour observed in going from plutonium to americium in the series are well documented and the subject of several reports. A few years ago the remarkable behaviour of americium under pressure[1] precipitated a strong interest in the behaviour of its 5f electrons and the structural changes observed. Very recently, both experimental and theoretical findings regarding curium under pressure were published; these findings demonstrated that curium's behaviour under pressure[2] was not a mirror image of that for americium. Rather, one of the five crystallographic phases observed with curium (versus four for americium) was a unique monoclinic structure whose existence was attributed to a special spin stabilization effect by curium's $5f^7$ electrons and its half-filled shell. These findings for curium have resulted in additional overall theoretical interest in these transplutonium metals, as their reduced atomic volumes affect the energies of the structures and the potential bonding that is present. In this presentation, we review briefly the behaviour of curium under pressure but also report on the behaviours of curium alloys under pressure relative to the behaviour observed with pure curium, and discuss the significance of the differences found.

RESULTS

Curium has a half-filled shell with seven 5f electrons spatially residing inside its radon core, and the element lies at the center of the actinide series. Compared to americium up to 100 GPa, curium exhibits one additional, unique structural form (identified as a Cm(III) phase, having a monoclinic symmetry) that occurs between 37 and 56 GPa. Ab initio electronic structure calculations agree with the observed experimental structural sequence[2], and these calculations also establish that it is the spin polarization and magnetism of curium's 5f electrons that are responsible for the formation and stabilization of this Cm (III) phase. With additional pressure, curium then adopts the Fddd and then the Pnma structures displayed by americium[1], as a result of acquiring additional participation of the 5f electrons in its bonding. The Pnma structures observed for americium and curium approaching 100 GPa are accepted as reflecting that full delocalization of their 5f electrons has occurred.

To enlighten further the influence of spin polarization for formation of the Cm (III) phase, as well as for the overall behaviour of curium, we consider here the pressure behaviours of curium alloys formed with its near neighbours, americium and berkelium: specifically, an $Am_{0.5}Cm_{0.5}$ alloy[3] and two Cm,Bk alloys ($Cm_{0.7}Bk_{0.3}$ and $Cm_{0.46}Bk_{0.54}$). The experimental relative volume (V/V_0) behaviours of americium, curium and the two Cm,Bk alloys are shown in Figure 1. The behaviour of the $Am_{0.5}Cm_{0.5}$ alloy under pressure[3,4] is similar to that for pure americium although the transitions are shifted to higher pressures. In all of these alloys under pressure, the unique Cm (III) phase is not observed.

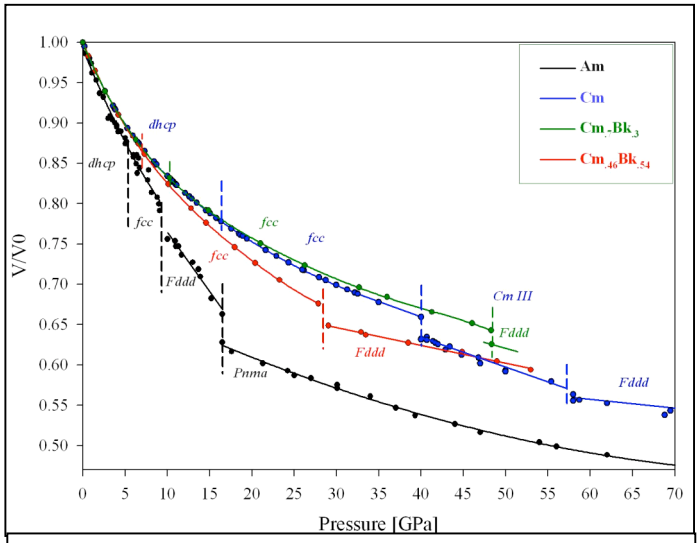

Fig. 1: The compression behaviours of Am, Cm and the two Cm,Bk alloys are displayed up to 70 GPa. (The Pnma structure for curium is observed above 90 GPa)

The crystal structures of the three alloys containing curium under pressure were considered by first-principles, self-consistent total energy calculations based on the generalized full potential, linear muffin-tin orbital (FPLMTO) method together with the generalized gradient approxiamtion by Perdew, Burke and Ernzerhof within density functional theory. The virtual crystal approximation and the spin-orbit coupling of the 5f-electrons are considered in the calculations for these alloys. Both antiferromagnetic and ferromagnetic calculations were performed for the different phases. The structural results found were in good agreement with experimental findings.

Acknowledgements

Support was from the European Commission, JRC, the Div. of Chem. Sciences, Geoscience and Bioscience, OBES, DOE with ORNL (DE-ACO5-00OR22725, UT-Battelle), the CEA and the Swedish Research Council & Swedish Foundation for Strategic Research**.**

References

1. S. Heathman et al, *Phys. Rev. Lett*., **85** (2000) 2961.
2. S. Heathman et al, *Science*, **309** (July, 2005) 110.
3. T. Le Bihan et al, *J. Nuc. Science Technol*., **Suppl. 3** (Nov. 2002) 45.
4. Sa Li et al, *Mat. Res. Soc. Symp. Proc.,* **893** (2006) 233.

Correlations Magnetism and Structure Across the Actinide Series:a Dynamical Mean Field Theory (DMFT) Perspective.

K. Haule* G. Kotliar * S. Savarsov† and A. Toropova*

- * Serin Physics Laboratory Rutgers University Piscataway NJ 08854-8019 USA.
  † Physics Department University of California Davis, CA 95616

In the early actinides the f electrons are well described by the itinerant model while in the late actinides they should be treated as localized.
Dynamical Mean Field Theory (DMFT), allows to treat localized and itinerant electrons within a unified approach, and properly describes the crossover between the two regimes.

We will present a comparative DMFT study of Pu[3], Am[2], and Cm[1].
We will discusss the photoemission and inverse phtoemission spectra of the different phases of these materials, and discuss the relation between structural properties electronic properties and magnetism in these materials.

Electron electron interactions are dominant for delta plutonium, while the phonon entropy has to be included for a proper description of the delta to epsilon transition. In all cases DMFT predicts a non magnetic ground state in agreement with experiments.
The theory predicts Cm to be magnetic, and predictions for the magnetic structure and the photoemission spectra of this material will be presented and compared with existing experimental data.

The Mott transition point, is located between Plutonium and Americium, and has very different character when approached from the Plutonium or the Americium side. Approaching the Mott point from the itinerant side, leads to an increase in the specific heat. The approach from the the localized side is accompanied by mixed valence and superconductivity.
In plutonium, the f-valence is between f^5 and f^6, while in Am under pressure, it is between f^6 and f^7. Cm has a nearly pure f^7 configuration.

We will conclude with a discussion of the implications of these results for alloys, and discuss the possible formation of local moments in these systems.

Acknowledgements: work supported by the Department of Energy.

1 K. Haule et.al in preparation..

2 S. Savrasov K. Haule and G. Kotliar PRL in press.
3 For a review see G. Kotliar et. al. Rev Mod Phys in press.

Plutonium and Quantum Criticality

G Chapline*, M. Fluss*

*Lawrence Livermore National Laboratory, Livermore CA 94552 USA

ABSTRACT

At its onset the Manhattan Project was bedeviled with a peculiar problem; the lattice structure and density of elemental Pu seemed to depend on how it was prepared. Perhaps even more remarkably, despite the great importance of this problem and the passage of more than 60 years, understanding why Pu occurs in these two allotropic forms has proved elusive. Adding to this enigma are many other puzzles such as why attempts to calculate the densities and binding energies of Pu from first principles seem to typically require that the Pu ions have local moments that are antiferromagnetically ordered, while there is considerable experimental evidence that there are no local magnetic moments in elemental Pu.

Fortunately a solution to these puzzles may be on the horizon. A hint that elemental Pu lies close to a quantum critical point (QCP) of some kind is that as a function of relatively modest changes in temperature and pressure there are a variety of complex phase transitions in Np, Pu, and Am that apparently involve changes in both the lattice structure and the electronic organization of the 5f electrons [1]. Consideration of atomic volumes suggests that it is δ phase of Pu that is nearest to the QCP point. Indeed, the negative thermal expansion of δ Pu for low impurity doping is by itself indicative of quantum critical behavior. A possible clue to the origin of the quantum critical behavior of Pu is provided by the pressure versus atomic volume curves for many rare earth materials that show a discontinuous decrease in volume at a critical pressure. In elemental Sm though this volume collapse becomes a continuous transition, and the proliferation of complex phases on the high pressure side of this transition is reminiscent of Am/Pu. Although these transitions occur at finite temperature the evolution of the first order volume collapse transition into a continuous transition as the atomic number of the rare earth approaches that of Sm is remarkably similar to the changes in P vs V curves of a quantum fluid near to zero temperature that result from changing some parameter in the Hamiltonian (cf Fig1). In general, for some particular value of the parameter there is no longer a discontinuous change in volume, but only a critical point. Very recently direct evidence has been obtained for the evolution of volume collapse in CeTh doped with La into a continuous transition at zero temperature as the La doping approaches 15% [2].

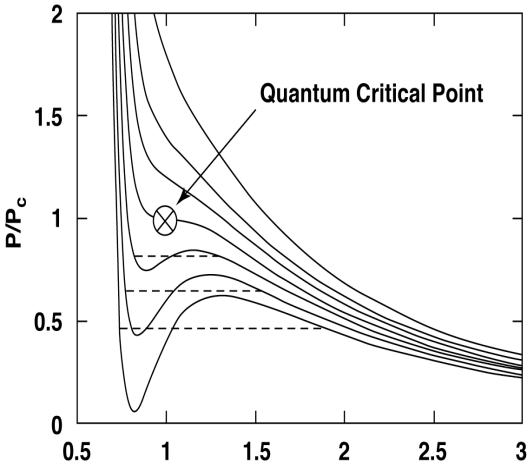

Fig 1: Pressure versus condensate density for a quantum fluid at zero temperature for various values of a parameter in the Hamiltonian such as the strength of repulsion between constituent particles.

An obvious question that arises in connection with associating the behavior of the elemental rare earths and actinides with a QCP is what is the physical nature of the organizational changes in the ground state? It cannot be a Mott metal-insulator transition because Mott transitions are always first order. In the case of the actinides it does not appear to be a change in magnetic order; although Np and Pu have rather large magnetic susceptibilities, neither are magnetic at accessible temperatures, while Am is superconducting at low temperature. The answer may be that in both the rare earths and actinides the metallic electrons form a "gossamer condensate"; i.e. the ground state wave function has BCS-like pairing of mobile charge carriers. The idea of a gossamer condensate was originally introduced to explain the close relationship between antiferromagnetism and high T_c superconductivity in the hole doped cuprates. Subsequently it was suggested [3] that there is a gossamer condensate in all materials that have metal → bad metal phase transitions similar to the $\alpha \rightarrow \gamma$ volume collapse transition in Ce. The presumed reason that these gossamer materials are metallic and not superconducting is that the quasi-particle excitation gap is very small. In this talk I argue that both the rare earth volume collapse transitions and the strange behavior of the actinides near to Pu have their origin in the presence of a gossamer condensate that is strongly coupled to the crystal lattice.

In a superconductor the condensate density is equal to the density of metallic electrons. In gossamer metals the spectral weight assigned to conduction electrons near to the Fermi surface is significantly reduced in comparison with ordinary metals due to electron repulsion. On the other hand decreasing the spectral weight of mobile electrons decreases the binding energy of the lattice. As a result of competition between the changes in spectral weight for conduction electrons and Fermi pressure the P vs V curve for a gossamer metal will be qualitatively similar to the pressure versus atomic volume curves for the elemental rare earths. The photoemission amplitudes will also behave at least qualitatively as observed for both elemental rare earths and actinides. In addition, the magnetic susceptibility near to the critical point will be quite large.

The physical origin of the gossamer condensate in rare earth and actinide materials may be spin orbit effects. It is well known that spin orbit effects are important for core states in f-electron materials. Spin orbit effects may also be important for conduction states if the screening length is not too small and lattice distortions give rise to a Rashba effect. Under these circumstances the charge carriers are localized and carry a monopole-like charge. The BCS-like pairing is a result of the fact that spin up and spin down carriers carry opposite monopole charge. The picture that emerges for impurity stabilized δ Pu is that it a mixture of two phases: a nearly uniform condensate with only transient distortions of the fcc lattice mixed with "gossamer insulae", where the condensate density is substantially larger and the lattice is permanently distorted. This phenomenon is similar to the occurrence of low temperature textures in the manganites, except that the δ Pu texture involves continuous variations rather than domain walls. Thus δ Pu provides a prototype for heterogeneous quantum ground states which occur because of proximity to a quantum critical point rather than a metal-insulator transition.

The authors are grateful to Scott McCall, Jason Lashley, and Jim Smith for discussions

1 G Chapline and J. L. Smith, LA Science **26,** 1 (2000).
2 J. C. Lashley, *to be published* .
3 G. Chapline, Z. Nazario, and D. Santiago, Phil. Mag. **85,** 867 (2005).

INSTABILITY OF ACTINIDE ELECTRON STRUCTURE UNDER HIGH PRESSURE

B.A. Nadykto

RFNC-VNIIEF, Arzamas-16 (Sarov), Nizhni Novgorod region, 607190,

E-mail:nadykto@vniief.ru, Fax: 83130 45772

1. Refs. [1], [2] show the course of transformation of four plutonium-gallium alloys with 1, 1.7, 2.5 and 3.5 at. % Ga under isostatic pressure at 25°C in Bridgman dilatometer. As expected, large-volume δ phase collapses at low enough pressures and transfers directly from δ to α′ phase with possible γ′-phase traces. Everything indicates that δ→α′ transformation proceeds by the martensite mechanism much like it has been found in cooling.

The data presented shows that when δ-phase alloy volume changes under applied positive pressure above a body the work is done which is expended for the δ→α′ transformation. This means that the energy level of the alloyed δ-phase is lower than that of the α′ phase. At the same time, it is well known that the unalloyed α phase is more beneficial energetically than the unalloyed δ phase and the transition from the α phase to the δ phase at room temperature occurs when tensile stresses of 0.35 GPa are applied [3].

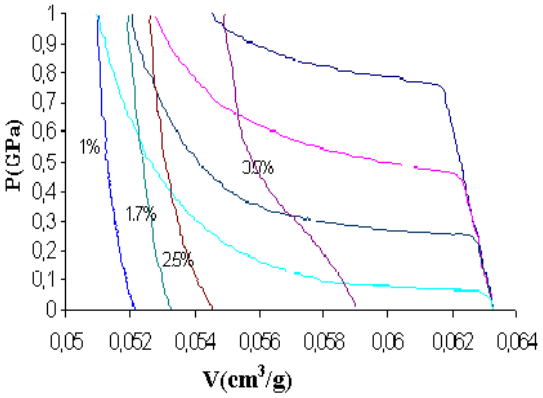

Fig. 1. Pressure versus specific volume of Pu-Ga alloy with different contents of Ga (at. %) in loading and pressure release

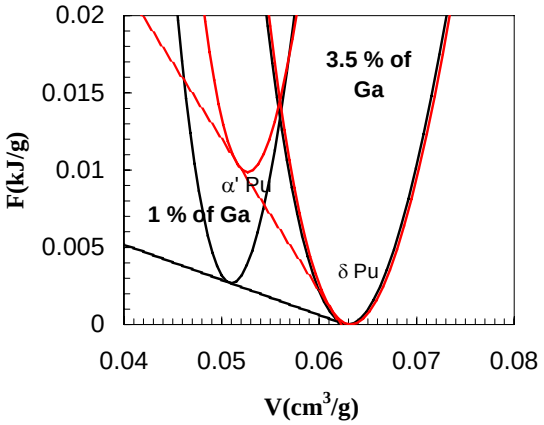

Fig. 2. Energy of α′ and δ plutonium alloys as a function of specific volume.

The presented curves can be used to determine from Fig. 1 the energy of the δ→α′ transformation as a function of gallium concentration in alloy through calculation of $\int PdV$ at the inelastic segment of the compression curve. Energy per gallium mole in alloy is almost independent of gallium content, which suggests the existence of some stable gallium complex in δ plutonium, which manifests itself identically in alloys with Ga content ranging from 1 at. % to 3.5 at. %. Energy of this complex can be represented as ΔE=67-100x kJ/mole Ga, where x is the relative fraction of Ga in Pu-Ga alloy. In this case the enthalpy of intermetallic compound Pu_3Ga is 42 kJ/mole, which is close to the data evaluated in the literature [4].

The pattern of the transition of gallium-alloyed δ-plutonium alloy under pressure to

the α′-phase state can be represented in the graph of Helmholtz free energy as a function of specific volume. Internal energy of different plutonium phases is given by

$$E_i(\sigma) = \frac{9B_i}{2\rho_i}(\sigma^{1/3} - 1)^2 + C_i,$$

where B_i and ρ_i are the bulk modulus and equilibrium density of each phase at standard conditions (at $\sigma = 1$), C_i are constants determining minimum energy for each phase. In Fig. 2, the calculation uses 30 GPa bulk modulus for δ phase, 50 GPa for α′ phase and experimental equilibrium densities of either phase. The slope of the common tangent to curves F(V) for the two phases determines the phase transition pressure in the thermodynamic equilibrium state.

The plots in Fig. 2 show that the transition occurs with changing pressure, and this is evidence of thermodynamic disequilibrium. The thermodynamic disequilibrium is also testified for by the presence of hysteresis. It is well known (at least, at elevated temperatures of 130-150 ^{o}C) that the remaining δ phase gets enriched in gallium during the δ→α′ transformation. This kinetic process can be responsible for the thermodynamic disequilibrium.

The α-plutonium tension of P= – 0.35 GPa [3] that fits the α→δ transformation in unalloyed plutonium at standard temperature is correspondent with the phase energy difference of 1.2 kJ/mole. This value is less significantly than TΔS in the α→δ transformation (3.6 kJ/mole at 300 K and ΔS=12 J/mole). Because of scarcity of information about the α→δ transformation in tension the transition energies in pure and alloyed plutonium cannot be compared, as the fraction of δ phase that therewith results is unknown. The transition from the α′ phase to the pure α phase may be attended with energy release from 3.6 to 10 kJ/mole depending on gallium concentration. This can be energy of pure α-phase lattice deformation in α′-phase formation due to gallium atom capture in random sites of the α-phase lattice. The α′ phase is known to be of a lower density than the pure α phase, that is its lattice is expanded.

If it is taken that in gallium-stabilized δ phase there is chemical bond of gallium and plutonium similar to that in Pu_3Ga, while in the α′ phase the chemical bond disappears, then Helmholtz free energy difference evaluated experimentally from the δ→α′ transformation under pressure at constant temperature is close to plutonium-gallium alloy formation enthalpy. Fig. 3 plots the δ plutonium alloy calculated enthalpy, divided by mole of the sum of nuclei of plutonium and complexes Pu_3Ga depending on atomic fraction of gallium in Pu-Ga alloy. Two experimental points obtained with the method of drop calorimetry [5] fall exactly on this calculated curve. In other words, the results of the measurements and experiments on the δ→α′ transformation under pressure agree. The results of drop calorimetry for Pu-Al alloy are presented in ref. [12].

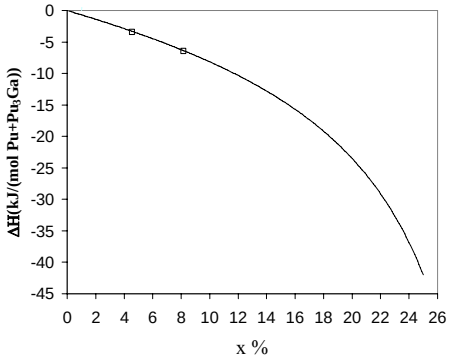

Fig. 3. δ plutonium alloy formation enthalpy (kJ/mole/(mole of Pu + Pu_3Ga)) versus Ga concentration in Pu-Ga alloy

2. The recent experiments using diamond anvils and synchrotron radiation sources have supplied interesting, important information about crystalline and electron structure of actinides in the megabar pressure range [6-10].

Ref. [7] studies compressibility of Pa to 129 GPa pressure. The computational analysis shows that up to P≈95 GPa the experimental points fall on the computed curve with parameters ρ_0 = 15.37 g/cm^3 and B_0 = 115 GPa. At higher pressures the experiment deviates significantly from the computed dependence and can be described as the state of another Pa electron phase with parameters ρ_0 = 19,827 g/cm^3 and B_0 = 400 GPa. Ref. [7] notes that at P=77 GPa the tetragonal structure of protactinium changes to low-symmetry orthorhombic structure of α uranium. At 77 GPa, however, there is no noticeable change in slope of the curve P(ρ), which is evidence that the initial electron structure of Pa remains unchanged. The slope and electron structure change abruptly at 95 GPa, evidently, at unchanged orthorhombic crystalline structure. Previously [11] it was noted that the experimental data on compressibility of thorium and uranium also indicated the existence of a stiff phase in them (with B_0=400 GPa) at pressure above 100 GPa.

Compressibility of curium metal to 100 GPa pressure is studied in ref. [10]. The parent phase of Cm (of equilibrium density 13.3 g/cm^3) has bulk modulus B_0 = 40 GPa, which is somewhat higher than that of americium metal and δ-phase plutonium. At pressure about 10 GPa the electron structure of Cm metal changes. The new phase parameters are ρ_0 = 13.96 g/cm^3, B_0 = 60 GPa. According to [10], at 17 GPa the parent dhcp structure changes to fcc structure. In the 10-37 GPa pressure range, however, the experimental points are described well as states of one electron phase. Phase CmIII (monoclinic structure) has somewhat lower bulk modulus (B_0 = 53 GPa) at the same equilibrium density (ρ_0 = 13.96 g/cm^3). For P>57 GPa the points for phases CmIV and CmV can be described as states of one and the same electron phase with ρ_0 = 20.35 g/cm^3, B_0 = 280 GPa. The parameters of this electron phase are close to those of phase Am IV at pressure 55-100 GPa.

At standard conditions, there are three electrons in the outer shell in thorium metal and four in uranium. In compression by high pressure the electron structure rearrangement takes place leading to the increase in the number of outer electrons to five or even six. In americium and curium the number of outer electrons increases under pressure to five.

References

1. S.S. Hecker, D.R. Harbur, T.G. Zocco. Phase stability and phase transformation in Pu-Ga alloys. //*Progress in Materials Science*. 49 (2004) 429-485.
2. S.S. Hecker, D.R. Harbur, T.G. Zocco. Phase stability in plutonium-gallium alloys. //Proceedings of International Workshop “Fundamental Properties of Plutonium”, Sarov, 30 August – 2 September 2004. P. 3.
3. S.S. Hecker. Plutonium and its alloys. // Los Alamos Science. 26. 2000. P. 290.
4. Химия актиноидов. Т. 2. Ред. Дж. Кац, Г. Сиборг, Л. Морсс. М.: Мир. 1997. С. 558-621.
5. Stan M., Baskes M.I., Muralidharan K., Lee T.A., Hu S., Valone S.M. Termodynamic properties of Pu-Ga alloys. // Fundamental Plutonium Properties. Abstracts of V International Workshop, September 12-16, 2005. Snezhinsk. Russia. P. 73-75.
6. Vohra Y.K., Akella J. Phys. Rev. Lett. 1991. V. 67. P. 3563
7. Haire R.G., Heathman S., Idiri M., Le Bihan T., Lindbaum A., Rebizant J. Phys. Rev., 2003, B**67**, 134101
8. Le Bihan T., Heathman S., Idiri M., Lander G.H. et al. Phys. Rev., 2003, B**67**, 134102
9. Lindbaum A., Heathman S., Litfin K. at al. // Phys. Rev. 2001. Vol. B63. 214101
10. Heathman S., Haire R.G., Le Bihan T., Lindbaum A. et al. // Science. 2005. Vol. 309. P. 110-113.
11. Nadykto B.A., Nadykto O.B. //Plutonium Future – Science 2003. Conference Transactions. Ed. by G.D. Jarvinen. Albuquerque. New Mexico, USA, July 6-10, 2003. P. 184-186.
12. Akhachinskiy V.V., Timofeeva L.F.// Thermodynamic of Nuclear Materials. 1979. Proc. of Sympos. Julix, 29 Jan. – 2 Feb. 1979. Vol. II. IAEA, Vienna, 1980. P. 161-169.